LIPASE-MEDIATED DEGRADATION OF POLY-ε-CAPROLACTONE IN TOLUENE: BEHAVIOR AND ITS ACTION MECHANISM

MUHAMMAD HAZIQ BIN ARIS

FACULTY OF SCIENCE
UNIVERSITY OF MALAYA
KUALA LUMPUR

2017

LIPASE-MEDIATED DEGRADATION OF POLY-ε-CAPROLACTONE IN TOLUENE: BEHAVIOR AND ITS ACTION MECHANISM

MUHAMMAD HAZIQ BIN ARIS

DISSERTATION SUBMITTED IN FULFILMENT OF THE REQUIREMENTS FOR THE DEGREE OF MASTER OF SCIENCE

INSTITUTE OF BIOLOGICAL SCIENCES
FACULTY OF SCIENCE
UNIVERSITY OF MALAYA
KUALA LUMPUR

2017

UNIVERSITY OF MALAYA

ORIGINAL LITERARY WORK DECLARATION

Name of Candidate : **MUHAMMAD HAZIQ BIN ARIS**

Matric No : **SGR 120017**

Name of Degree : **MASTER OF SCIENCE**

Title of Project Paper/Research Report/Dissertation/Thesis ("this Work"):

LIPASE-MEDIATED DEGRADATION OF POLY-ε-CAPROLACTONE IN TOLUENE: BEHAVIOR AND ITS ACTION MECHANISM

Field of Study : **BIOTECHNOLOGY**

I do solemnly and sincerely declare that:

(1) I am the sole author/writer of this Work;
(2) This Work is original;
(3) Any use of any work in which copyright exists was done by way of fair dealing and for permitted purposes and any excerpt or extract from, or reference to or reproduction of any copyright work has been disclosed expressly and sufficiently and the title of the Work and its authorship have been acknowledged in this Work;
(4) I do not have any actual knowledge nor do I ought reasonably to know that the making of this work constitutes an infringement of any copyright work;
(5) I hereby assign all and every rights in the copyright to this Work to the University of Malaya ("UM"), who henceforth shall be owner of the copyright in this Work and that any reproduction or use in any form or by any means whatsoever is prohibited without the written consent of UM having been first had and obtained;
(6) I am fully aware that if in the course of making this Work I have infringed any copyright whether intentionally or otherwise, I may be subject to legal action or any other action as may be determined by UM.

Candidate's Signature Date:

Subscribed and solemnly declared before,

Witness's Signature Date:

Name:

Designation:

ABSTRACT

Poly-ε-caprolactone (PCL) is a semi-crystalline polyester, hydrophobic in nature and highly degradable. However, these properties make it unsuitable for many applications. Blending of PCL oligomers with other polymer(s) helps to improve its characteristics. It is suggested that by degrading the long PCL chain into moderate length would permit the blending and functionalization processes to be more amenable to control variables. In this study, lipase-catalyzed hydrolysis of PCL in toulene was investigated. PCL with number-average molecular weight (M_n) 10,000 g mol^{-1} was hydrolyzed using immobilized *Candida antarctica* lipase B (CALB). The increase in PCL concentration led to a decrease in degradation rate. Enhanced rate was observed when reaction temperature was increased from 30 to 50 °C. Enzymatic chain scission of PCL yielded cyclic dicaprolactone, tricaprolactone, tetracaprolactone and oligomers with M_n less than ~ 1000 g mol^{-1}. Catalytic formation of cyclic lactones *via* back-biting mechanism in low water content environment was attributed to CALB. Its hydrolysis of PCL displayed consecutive random- and chain-end scission with time from detailed thermal, molecular weight and structural analyses. Apparent activation energy, E_a for hydrolysis was 45 kJ mol^{-1} i.e. half of that reverse reaction. Dicaprolactone and oligomers from hydrolysis readily re-polymerized to produce mid-range polymer with M_n 1400 g mol^{-1} after 36 hours in the same reaction medium. These versatile oligomers can be applied as integral components for processes such as copolymerization or functionalization of valuable compounds.

ABSTRAK

Poly-ε-caprolactone (PCL) adalah polyester yang bersifat separa kristal, hydrofobik secara semula jadi dan mudah terurai. Walaubagaimanapun, sifat-sifat fizikal ini tidak sesuai untuk kebanyakan aplikasi. Penggabungan oligomer dengan polimer lain dapat membantu untuk memperbaiki ciri-cirinya. Pemotongan rantai panjang PCL kepada sederhana panjang membuatkan proses penggabungan dan functionalization antara polimer lebih mudah dan perubahannya boleh dikawal. Kajian mengenai Lipase sebagai pemangkin hydrolisis polycarolactone dalam toluene telah dijalankan. PCL yang mempunyai nombor purata berat molekul (M_n) 10,000 g mol^{-1} telah dihydrolisis menggunakan immobilized *Candida antarctica* lipase B (CALB). Pertambahan kepekatan PCL menyebabkan kadar degradasi menurun. Peningkatan kadar degradasi dapat diperhatikan apabila suhu tindak balas kimia meningkat daripada 30 kepada 50 °C. Kesan pemotongan rantaian PCL oleh CALB menghasilkan cyclic dicaprolactone, tricaprolactone, tetracaprolactone dan oligomer dengan M_n kurang daripada ~1000 g mol^{-1}. Pembentukan cyclic lactones melalui mekanisma 'back-biting' dimangkinkan oleh CALB dalam persekitaran yang rendah kandungan air. Hydrolisis PCL menunjukkan CALB memotong secara rawak dan di bahagian akhir rantaian polimer secara berturutan dengan masa berdasarkan analisis haba, berat molekul dan struktur polimer. Tenaga pengaktifan hydrolysis, E_a adalah 45 kJ mol^{-1} iaitu separuh daripada reaksi terbalik. Selepas 36 jam, dicaprolactone dan oligomer digunakan kembali oleh CALB untuk proses polymerization menghasilkan polymer yang mempunyai berat molekul, M_n 1400 g mol^{-1} dalam medium tindak balas yang sama. Oligomer serba guna ini boleh digunakan sebagai komponen penting untuk proses seperti copolymerization atau functionalization sebatian yang berharga.

ACKNOWLEDGEMENT

Praise is to ALLAH for lighten us to see His greatness through His creation. There are so many people to thank for helping me during my master study. First, I would like to dedicate this work with love to my parents, Aris Bin Abdullah and Ngaisah Binti Mohd Yusof. At the same time, I am indebted to my supervisor Professor Mohamad Suffian Mohamad Annuar for trusting me with this work, guiding and correcting various documents of mine with attention and care. He has taken pain to go through the study and make necessary correction when needed. I would like to thank Professor Ling Tau Chuan for his financial support during my research study.

I would like to express the deepest appreciation to Dr. Ahmad Gumel, Nurul Nadiah, Maryam Farhana, Naziz, Faezah Ansari, Syairah Anis, and Haziqah for helped me in providing technical support, guidance and as well as encouragement. It is my privilege to thank Miss Zara, for the unending support in making this research possible.

Lastly, my thanks to Universiti of Malaya for the research grant and for the financial support via University Malaya Fellowship Scheme. Furthermore, I extend my gratitude to those who directly or indirectly had supported me during my research studies.

TABLE OF CONTENTS

LIST OF FIGURES

LIST OF TABLES

LIST OF SYMBOLS AND ABBREVIATIONS

PCL	Poly-ε-caprolactone
mcl-PHA	Medium chain length-polyhydroxyalkanoates
CALB	*Candida antarctica* lipase B
THF	Tetrahydrofuran
DCM	Dichloromethane
DSC	Differential scanning calorimetry
GCMS	Gas chromatography mass spectrometry
GPC	Gel permeation chromatography
TGA	Thermogravimetric analysis
kDa	kiloDalton
M_n	Number-average molecular mass
M_w	Mass-average molecular mass
T_d	Degradation temperature
T_m	Melting temperature
$[\eta]$	Intrinsic viscosity
R_h	Hydrodynamic radius
R_G	Radius of gyration
ξ	Screening length
ΔH	Enthalpy changes
ΔS	Entropy change
ΔG	Gibbs energy change
R^2	Correlation coefficient
R^2 adjusted	Adjusted correlation coefficient

CHAPTER 1

INTRODUCTION

Excellent progress has been made in the application of degradable polymers like poly-ε-caprolactone (PCL) as tissue-growth scaffolds (Reed *et al.*, 2009; Van Lieshout *et al.*, 2006), scaffold component for tissue engineering (Li *et al.*, 1990a; Rentsch *et al.*, 2009; Williamson & Coombes, 2004), anti-adhesion film (Lo *et al.*, 2010), suture coating (Yang *et al.*, 2002), drug delivery devices (Pitt *et al.*, 1987) and food packaging (Siracusa *et al.*, 2008) because of its biocompatible and non-toxic properties (Arote *et al.*, 2007). Unlike natural polymer, cells cannot assimilate most synthetic polymers because the degraded products are found to be toxic to them (Gupta *et al.*, 2002; Zeng *et al.*, 2004). Although PCL exhibits attractive properties, being hydrophobic in nature made it unsuitable for many applications. Meanwhile, blending of PCL with other polymer(s) helps to improve its characteristics (Chen *et al.*, 1982; Gupta *et al.*, 2002; Rittié & Perbal, 2008). It is recommended that the long PCL chain to be fragmented into moderate length prior to blending and functionalization processes, which allows for more amenable and controllable variables (Giri *et al.*, 2001).

It was demonstrated that lipase possesses wide substrate specificity with the ability to hydrolyze PCL in aqueous solution (Chen *et al.*, 1982). This has been demonstrated in a small scale but has yet to become viable for industrial application because of its low yield, enzyme reusability and cost issues. Furthermore, there is an outstanding issue of the very low solubility of hydrophobic PCL in the aqueous solution (Giri *et al.*, 2001). The use of immobilized enzyme for PCL degradation in organic solvent is a promising route in improving reaction kinetic, increasing the yield of degradation products and ease in products separation compared to aqueous mixture

(Arote *et al.*, 2007; Zaks & Klibanov, 1985). More importantly, PCL is more soluble in the organic solvent than aqueous solution (Coulembier *et al.*, 2006).

Since many enzyme kinetic studies involve soluble substrates reactions, Gumel *et al.* (2013) devised two immiscible solvents solution as a mixed medium in lipase-catalyzed esterification of 6-*O*-glucosyl-poly(3-hydroxyalkanoate) in order to improve polymer dissolution. Yet, single-type, dry organic solvent as reaction medium could be a viable solution to the solubility issue since immobilized enzyme such as CALB still contains about 1 wt % water (Deniz & Chang, 2000; Singh *et al.*, 2000; Uyama & Kobayashi, 2006) for it to perform degradative catalysis in organic solvent. This nominal amount of water is hypothesized to be sufficient for the enzyme to favor the hydrolysis of PCL as long as aqueous microenvironment on the surface of enzyme is not stripped away by the organic solvent (Kula, 2008). Paravidino *et al.* (2012) reported that non-polar solvent environment resulted in reduced flexibility of CALB in the core and the active site but higher flexibility for residues located on the surface. Proper selection of reaction medium for CALB is very crucial since five surface elements of CALB consisted of a short α-helix (residues 139-150), a long α-helix (residues 266-289) that forms the entrance to the active site, and three surface loops (residues 26-30, 92-97 and 215-222) exhibiting solvent-dependent flexibility change. Non-polar solvents do not alter the backbone and the total surface area of CALB but hydrophilic surface exposure is significantly decreased compared to when CALB is in aqueous environment (Rudd *et al.*, 1984). The reduction of hydrophilic surface of CALB in non-polar solvent concomitantly increases the exposure of its hydrophobic surface, which is expected to improve the enzyme binding with hydrophobic PCL.

It has been reported previously that both lipase and acid hydrolysis randomly cut at the PCL polymer backbone but lipase scission generated specific molecular sizes of oligomers than acid hydrolysis (Kobayashi & Makino, 2009). Therefore, an

investigation on the enzymatic depolymerization of PCL in non-aqueous medium was carried out to better understand the scission mechanism responsible and its reaction behavior in the course of generating shorter fragments.

In this study, the investigation will address the following objectives:

- To investigate the lipase-catalyzed depolymerization of PCL in toluene;
- To study the scission models in the lipase-catalyzed process;
- To provide mechanistic explanation of lipase action towards PCL in toluene.

CHAPTER 2

LITERATURE REVIEW

2.1 POLY-Ɛ-CAPROLACTONE

In the last decades, a remarkable increase in the use of petroleum based plastics and their environmental impact due to inappropriate disposal or incineration leading to important environmental problems such as soil contamination and toxic gas emission form incineration processes. This acts as driving force to the development and use of biodegradable plastics. Poly-ε-caprolactone (PCL) is well known biodegradable polyester, with semi-crystalline properties (Figure 2.1). It is a linear polyester that possesses hydroxyl groups on one end and carboxyl group on the other end of the polymer chain as in Figure 2.2 (Li *et al.*, 1990a, 1990b). PCL has been used in scaffold for tissue engineering (Christopher *et al.*, 2008; Matsumura, 2006; Plackett *et al.*, 2006b), anti-adhesion film (Lo *et al.*, 2010), suture coating (Barber & Click, 1992; Griebenow & Klibanov, 1996), drug delivery (Pitt *et al.*, 1987) and food packaging (Plackett *et al.*, 2006b) because they are biocompatible and non-toxic (Engelberg & Kohn, 1991).

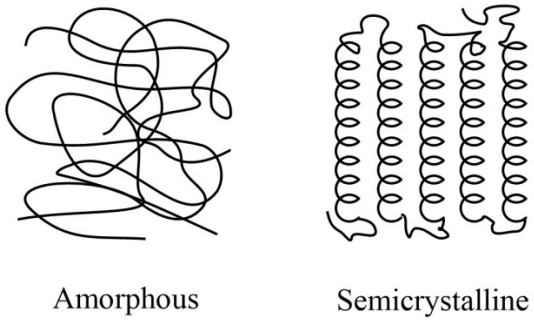

Figure 2.1. Semi crystalline structure of poly-ε-caprolactone

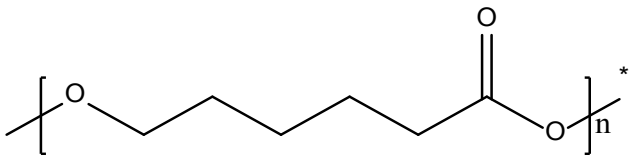

Figure 2.2. Structure of poly-ε-caprolactone

In the field of tissue engineering, researchers realized the importance of biodegradable polymers for building scaffolds to assist cell attachment, proliferation and functioning. These biodegradable polymers can be futher modified *via* physical or chemical methods but enzyme-mediated process is seen as specific, mild and environmentally-friendly method (Gumel *et al.*, 2015). Attractive properties of thermoplastic PCL are its non-toxicity, high decomposition temperature of 350 °C (Gopferich, 1996), low glass transition (-62 °C), low melting point (57 – 64 °C) and low unit price (Deniz & Chang, 2000). Since its natural properties made it unsuitable for many applications, blending of PCL with other polymers helps to improve its characteristics such as PCL blends with polylactic acid (PLA) (Patrício *et al.*, 2013), PCL blends with starch (Hubackova *et al.*, 2013) and PCL blends with polyethylene oxide (PEO) (Li *et al.*, 2014).

Another important characteristic is its dissolution behavior in solvents. At room temperature, PCL is soluble in dichloromethane, chloroform, toluene, carbon tetrachloride, benzene, cyclohexanone and 2-nitropropane. PCL is less soluble in ethyl acetate, dimethylformamide, acetonitrile, acetone, 2-butanone, and it does not dissolved in alcohol, petroleum ether, and diethyl ether (Siracusa *et al.*, 2008).

2.2 POLYMER IN DILUTE SOLUTIONS

It is crucial to obtain information on the behavior of polymer molecules in selected solvents due to the different dimensions involved between them. Firstly, the solvent molecules diffuse through the polymer matrix to form a swollen, solvated mass

called a *gel.* In the second stage, the gel breaks up and the molecules dispersed into a true solution (Huang, 1995). The size or the hydrodynamic volume of the polymer molecules in solution varies according to the type of solvents. Some polymers dissolve readily in certain solvents, others require heating at temperature near the melting point of the polymer. There are several factors affecting the hydrodynamic volume including interaction between solvent and polymer molecules, chain branching, conformational effects arising from the polarity and steric bulk of the substituent groups and restricted rotation caused by resonance. Generally, the average shape of the coiled molecules is spherical. Larger sphere denotes greater affinity by the solvent for the polymer. In dilute solution, strong polymer-polymer interactions are replaced by the weaker polymer-solvent interactions (Li *et al.*, 1990a). Mark-Houwink-Sakurada equation is used to relate solution viscosity to molecular weight.

$$[\eta] = KM_v^a \tag{2.1}$$

where $[\eta]$ is intrinsic viscosity, M_v is viscosity average molecular weight and α is a constant that varies with polymer, solvent and temperature. All the values can be obtained by graphical method of a plot of log $[\eta]$ versus log M_v or log M_n. Log K and a are the intercept and slope of the curve.

$$\log[\eta] = \log K + a \log M_v \tag{2.2}$$

Viscosity average molecular weight lies between M_n and mass-average molecular weight, M_w. For most common polymers, values of a vary between 0.5 (for a randomly coiled polymer in a theta solvent) and 0.8; for more rodlike extended-chain polymers where the hydrodynamic volume is relatively large, a may be as high as 1.0, in which case $M_v = M_w$. Chain entanglement not usually a problem at such high dilution unless molecular weights are extremely large (Li *et al.*, 1990b).

The main problem with molecular weight determination is when one is dealing with polymer other than commercial standard samples e.g. branching polymer instead of linear chain of polystyrene. The absolute molecular weight average can be determined *via* size exclusion chromatography coupled with differential refractive index, viscosity and light scattering (low angle and right angle). Data obtained from triple-detector size exclusion chromatography can be utilized to construct the universal calibration method. In the universal calibration method, the product of ($[\eta]M$) is called the universal calibration parameter. The basis of universal calibration is product of intrinsic viscosity (limiting viscosity number) and molecular weight is independent of polymer type. An approximately linear correlation of log ($[\eta]M$) against elution volume in solvent for dissimilar group of polymers can be obtained as follows:

$$[\eta]_{PS}M_{PS} = [\eta]_2 M_2 \tag{2.3}$$

From the Mark-Houwink-Sakurada relationship,

$$[\eta]_1 = K_{PS}{M_{PS}}^{a} \tag{2.4}$$

$$[\eta]_2 = K_2{M_2}^{a} \tag{2.5}$$

Combining these equations and solving for log M_2, we obtain

$$\log M_2 = \left(\frac{1}{1+a_2}\right)\log\left(\frac{K_{PS}}{K_2}\right) + \left(\frac{1+a_{PS}}{1+a_2}\right)\log M_{PS} \tag{2.6}$$

To measure M_2 accurately, the column must be calibrated with the standard polystyrene (PS) fractions with same solvent and temperature. From semi-logarithmic calibration plot of molecular weight versus retention volume, a linear plot at broad range of molecular weights can be observed except deviations from linearity at high and low molecular weights. Table 2.1 shows K and α values for MCL-PHA (Plackett *et al.*, 2006a). This method is convenient to calculate accurate absolute molecular weight average for polymer of interest M_2. The benefit of this calculation is that the absolute polymer molecular weight can be determined despite using a single detector. Despite

many available Mark-Houwink parameter in polymer handbook, it is necessary to select narrow range of molecular weight dispersion (MWD) rather than exponential MWD with M_w/M_n = 2.0, because bigger MWD will lead to an overestimate of molecular weight (Garcia-Alles & Gotor, 1998).

Table 2.1. Mark-Houwink calibration constants calculated from best fit of the data obtained by triple detector analysis of MCL-PHA samples in THF [$(\eta)=K(\mathrm{MW})^a$]

	A	Log (K/dL g^{-1})	MW (kDa)[b]
PS	0.716	-3.943	100
Universal PHA	0.689	-3.78	96.2

[b] Calculated for PS equivalent MW of 10^5 Da. Data obtained from Plackett *et al.* (2006a)

2.3 POLYMER IN CONCENTRATED SOLUTIONS

According to Lo *et al.* (2010), dilute solution is defined as a concentration where the product of the intrinsic viscosity [η] multiplied by the concentration c is less than one, and the polymer molecule acts as an isolated chain. When the product [η]c falls between 1 and 4 as the polymer concentration increases, polymer-polymer intermolecular interactions influence the motion of the polymer. The moderately concentrated region (the upper limit is [η]c = 4) would be expected to extend from the point where hydrodynamic flow is close to lamellae to a point where the polymer completely fills the solution, but does not lead to significant inter-penetration of the volume occupied by a neighbouring polymer molecule (Figure 2.3). A characteristic screening length, ξ denotes the juxtaposition of hydrodynamic interactions. At higher concentrations, [η]c = 10, formation of pseudo-matrix-gel due to coil-coil inter-penetration resulted from dynamic contacts is replaced by inter-coil contact. The higher limit [η]$c \approx 10$ can be considered as being indicative of entanglement formation.

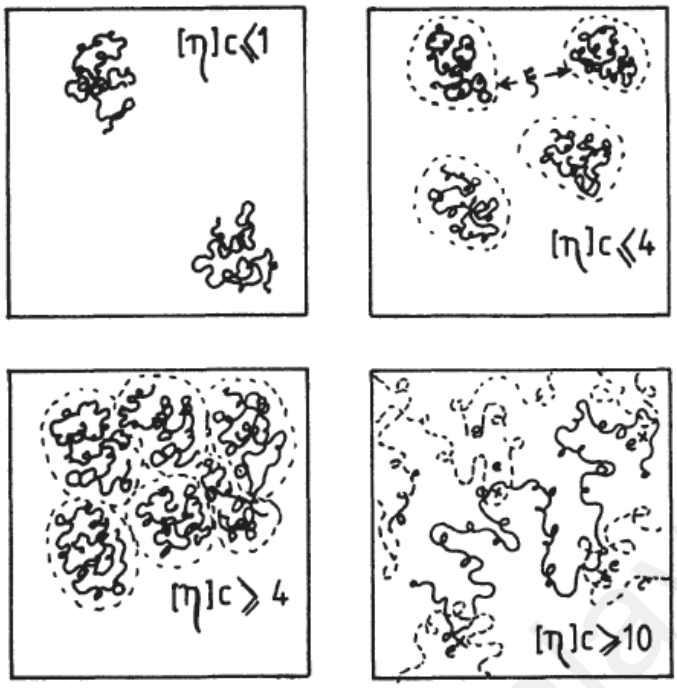

Figure 2.3. Polymer arrangement followed the Frisch and Simha regions of polymer-polymer interaction which [ŋ] represent intrinsic viscosity in dL g^{-1}; *c* represent the concentration of polymer in g dL^{-1}; dotted circles represent the effective volume occupancy of a polymer coil; ξ is the screening length; dashed lines represent the surrounding polymer matrix; *e* represent a point of entanglement. This diagram was reproduced from Yang *et al.* (2002).

In high molecular weight polymers, interactions between elements within the same chain lead to the so-called "excluded-volume" effects (Barber & Click, 1992). To explain the consequence of this effect, we can use adsorption of free polymer molecules on the colloid surfaces proposed by Bose *et al.* (2004) as a model for immobilized enzyme attack towards polymer chain. To illustrate this proposition, a schematic representation using colloidal particle of radius *R* and radius of gyration, R_G in a dilute polymer solution as shown in Figure 2.4 (a) is utilized. The colloidal particles have a spherical exclusion surface of radius ($R+R_G$) for the polymer molecules, and the centers of the non-adsorbing polymer molecules cannot enter this surface. R_G is refer to an average measure of the size of the macromolecule. Static light scattering (SLS) can be used to measure R_G. The term *R* is also the radius of gyration but it is a measure of the

hydrodynamic size of a polymer as it drifts through a fluid. The one of the instruments that can measure *R* is dynamic light scattering (DLS).

The exclusion surfaces overlap occur when the distances between the surfaces of the particles is less than the radius of gyration of the polymer. The polymer is excluded from the region between the particles. As a result, there is no osmotic pressure due to the polymer on the surfaces from which the polymer is excluded. Nevertheless, there is an osmotic pressure on the outer surfaces where the polymers surround the particles. Hence, there is a force of attraction which is proportional to the osmotic pressure times the cross-sectional area *S* of the region from which the polymers are excluded. The potential is the calculated by integration of the force variable with respect to distance (Bose *et al.*, 2004).

The representation can be made more general using smaller spherical particles in place of the polymer molecules as shown in Figure 2.4 (b). If the distance between the surfaces of the larger particles is smaller than the diameter of the smaller particle, the smaller particles are excluded from the region between the larger particles, and there is no osmotic pressure due to the presence of smaller particles in the region between the larger particles. Yet, there is still an osmotic pressure on the outer surfaces due to smaller particles, and this causes an attractive force if the pressure and the area of cross-section of the region from which the smaller particles are excluded. Since the pressure is not a constant, a slightly more complicated integration function of the force variable with respect to distance is expected. Finally, it should be noted that the present configuration is two-dimensional, so that the equivalent of the surface area *S* for colloidal particles is just a line segment (denoted by *h*) in two dimensions.

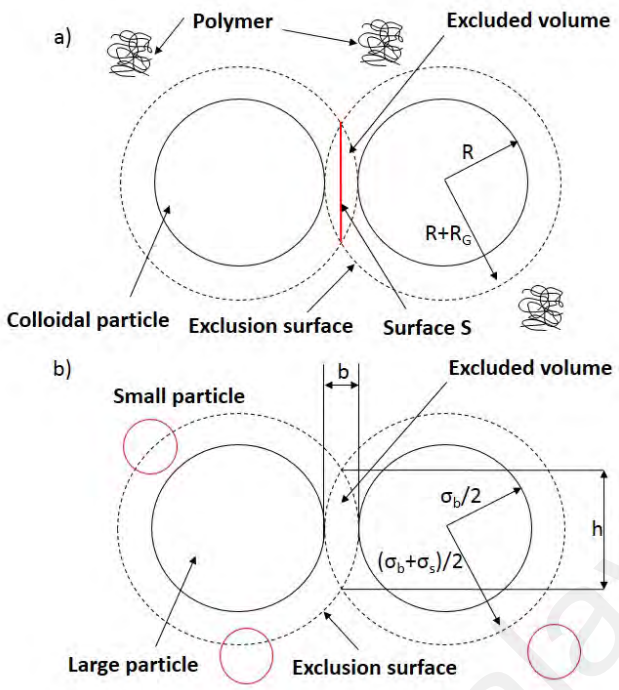

Figure 2.4. The excluded-volume attraction in colloidal particles (a) and between particles in a two-dimensional granular medium (b). (a) shows the overlap surfaces between exclusion surface with radius $R+R_G$ around a colloidal particle of radius R, and the cross-sectional area S of the excluded volume. The attractive force between the particles is the osmotic pressure due to the polymer times the surface area S. In (b), the region of width h is excluded to small particles, where $b = \sigma_b + \sigma_s - \alpha$ and $h = \sqrt{(\sigma_b + \sigma_s)^2 + \alpha^2}$ and σ_b and σ_s are the diameters of the large and the small particles, respectively (Bose *et al.*, 2004).

The combined theories by Gopferich (1996) and Bose *et al.* (2004) can be applied to guide our understanding on the behavior of Novozyme 435-mediated scission of PCL in toluene particularly on the observation that the enzyme degrades PCL *via* end chain scission only after higher molecular weight of PCL (M_n = 93 000 g mol^{-1}) was used as substrate (Desai *et al.*, 2004). This is despite reported random chain scission by other researchers when different initial molecular weights of PCL were used e.g. M_n = 60 000 g mol^{-1} by Tamada and Langer (1993) and M_n = 40 000 g mol^{-1} by Ansari and Amirul (2013) in the same solvent under similar conditions. The observed behavior is attributed to the inter-chain interaction between pairs of high molecular weight coils. As shown in equation (2.7) obtained from Halling (1984), there is a correlation between molecular weight, intrinsic viscosity and hydrodynamic radius (R_h) of polymer. In

addition, inverse intrinsic viscosity provides information regarding molecular density of polymer. When high molecular weight chains (M_n = 93 000 g mol^{-1}) is used as degradation substrate, the intrinsic viscosity subsequently increase therefore the polymer become less tightly coiled, leading to the increment of R_h. Bigger R_h makes the polymer coil to inter-penetrate with particle nearby it creating an excluded-volume. The presence of excluded volume prevents the enzyme from accessing the polymer backbone. Thus, only the exposed chain-ends are susceptible towards enzyme attack. However, Kondo *et al.* (2002) obtained random chain scission at higher initial molecular weight PCL (M_n = 110 000 g mol^{-1}) when the experiment was conducted under 18 MPa pressure in supercritical carbon dioxide. Additional pressure applied and different solvent used could have caused changes in the PCL conformation. The microstructural changes are attributed as the primary reason more ester bond in the polymer chain to be exposed for random enzymatic scission.

$$[\eta]M = \frac{10}{3}\pi \cdot R_h^3 \tag{2.7}$$

2.4 ADVANTAGES OF ENZYME CATALYSIS

Enzymes have been used extensively in molecular biology (Stevens, 2009), biochemical studies (Santaniello *et al.*, 1993), and biotransformation. Biotransformation includes chemical reactions catalyzed by cells, organs or enzymes. The unique properties of biocatalysts are their stereo- and regiospecificity, and their ability to undergo reactions at mild pH and temperature (Yadav & Devi, 2004). Enzymes exhibit enantioselectivity reacting with only one isomer, and regioselectivity preferentially reacting with only one site on a molecule despite multiple sites of potential reactions (Alexander, 2001).

Kawata and Ogino (2009) have discovered that lipases can act as catalysts in a number of nearly anhydrous organic solvents. This discovery brought new perspective in this field and surpasses the limit of traditional enzymes reaction, which restricts the catalytic activity only in aqueous solution. The breakthrough widens the applications of enzyme catalysis especially in polymer synthesis since most of polymer are hydrophobic in nature and only dissolve in organic solvents. New directions of synthesis are emerging with respect to condensation (Kamal *et al.*, 2013), ring-opening (Alexander, 2001) and controlled free radical polymerization (Gumel *et al.*, 2011).

Furthermore, there are several advantages compared to chemical preparative routes. Enzymes, derived from renewable resources have 1) promising substrate conversion efficiency due to high selectivity for a given organic transformation; 2) high enantio- and regioselectivity; 3) catalyst recyclability; 4) can be used in bulk reaction media avoiding organic solvents and; 5) represents an important option in meeting environmental regulation (Kula, 2008; Zaks & Klibanov, 1985). Their extended uses in organic or aqueous systems or the solventless system and specificity of the reaction have made them particularly attractive to replace toxic heavy metal in polymer synthesis (Alexander, 2001). Enzymatic catalysis in polymer science has thrived in recent years and has been discussed reviewed in recent literature (Matsumura, 2006; Wang *et al.*, 2007).

Previously, wider application of lipase has been limited because of this enzyme was thought to work effectively only in high water contents and would rapidly lose its activity in organic solvents (Kamal *et al.*, 2013). Later, the enzyme was found to remain active in organic solvents, and this generated huge interest among researchers and industries since most of the industrial substrates are hydrophobic. Furthermore, the solvent helps prolonged enzyme activity by replacing the molecules of water in the enzyme with solvent and this simultaneously enable the reactions impossible in water

such as esterification to be carried out (Garcia-Alles & Gotor, 1998; Wang *et al.*, 2007). Usually, reaction in water pose difficulties in the separation of enzyme and product(s) but in an organic solvent medium, enzyme is insoluble and this facilitates product recovery (Segel, 1976).

2.5 PROPERTIES OF LIPASE AND ITS HYDROLYSIS MECHANISM

Lipases are classified as triacylglycerol acylhydrolases (EC 3.1.1.3). Lipases are stereospecific towards ester bond and simultaneously, undesirable by-products is eliminated (Gupta *et al.*, 2002). Lipase has been extensively use as biocatalyst in industries because its higher stability at high temperatures, able to tolerate wide range of pH and immobilized lipases can be repeatedly use e.g. Novozyme 435 (CALB) (Wood *et al.*, 1965). Lipase also one of the most versatile enzymes because they can catalyze many different reactions such as esterification, inter-esterification, hydrolysis, alcoholysis, peroxidations, aminolysis, and epoxidations (Wood *et al.*, 1965). According to Annuar *et al.* (2008), selectivity is related to chemo-selectivity i.e. the the favoured reaction of a substrate with one of two or more different functional groups; regioselectivity i.e. the position in the substrate molecules of the ester bonds hydrolysed or formed, and stereoselectivity i.e production of single enantiomers instead of racemic mixtures (Reed *et al.*, 2009). On the other hand, specificity (k_{cat}/K_m) can be defined as the ratio of catalytic constant (k_{cat}) and Michaelis constant (K_m) (Wood *et al.*, 1965).

Candida antarctica lipase B (CALB) is made up of 317 amino acid residues having a formula weight of 33,273. The active centre has a catalytic triad, serine (Ser105), histidine (His224), aspartic acid (Asp187) with a large hydrophobic pocket above the Ser-His-Asp triad and a medium-sized pocket below it. During the catalysis, the acyl moiety of the substrate lies in the large subsite, while the leaving group/nucleophile moiety lies in the medium-sized pocket (Kobayashi, 2010).

Engelberg and Kohn (1991) reported that in Novozyme 435 where crude CALB (SP 525) is immobilized on a macroporous acrylic resin, the lipase protein content constituted 2 % (w/w) of the solid powder (40 % of the total protein content).

Kaufman (1990) proposed a charge-relay system to explain the mechanism of catalytic triad *Asp-His-Ser* as in Figure 2.5. Annuar *et al.* (2008) stated that hydrolysis of lipid consists of two steps. The reaction begins with the formation of hydrogen bond between the aspartic acid group (*Asp*) with histidine (*His*), increasing the pK_a and then acting as a powerful general base. The proton transfer on either one of two nitrogen atoms in the *His* ring allows serine to transfer proton to the catalytic triad to form an oxyanion ion. This reactive nucleophile is capable of attacking the susceptible ester bond to form a tetrahedral intermediate carrying a negative charge on the carbonyl oxygen atom of the scissile bond. Phenylalanine (*Phe*) and leucine (*Leu*) residues help to stabilize the charge in the oxyanion hole. Next, *His* moiety donates a proton to the ester oxygen of the bond that is cleaved and forms intermediate with the fatty acid from the substrate esterified to serine (*Ser*). Simultaneously, the carbonyl group reforms with the glycerol backbone segment acting as the leaving group. The second step of the reaction is deacylation of the enzyme through a water molecule that cleaves the acyl-enzyme intermediate. In this case, a proton from water molecule is transfer to the active site serine producing a reactive hydroxide ion that attacks the carbonyl carbon atom in the substrate-enzyme covalent intermediate. The second negatively charged tetrahedral intermediate is stabilized *via* hydrogen bonds to oxyanion hole. Finally, *His* transfers a proton to the oxygen atom of *Ser* and the acyl component is released.

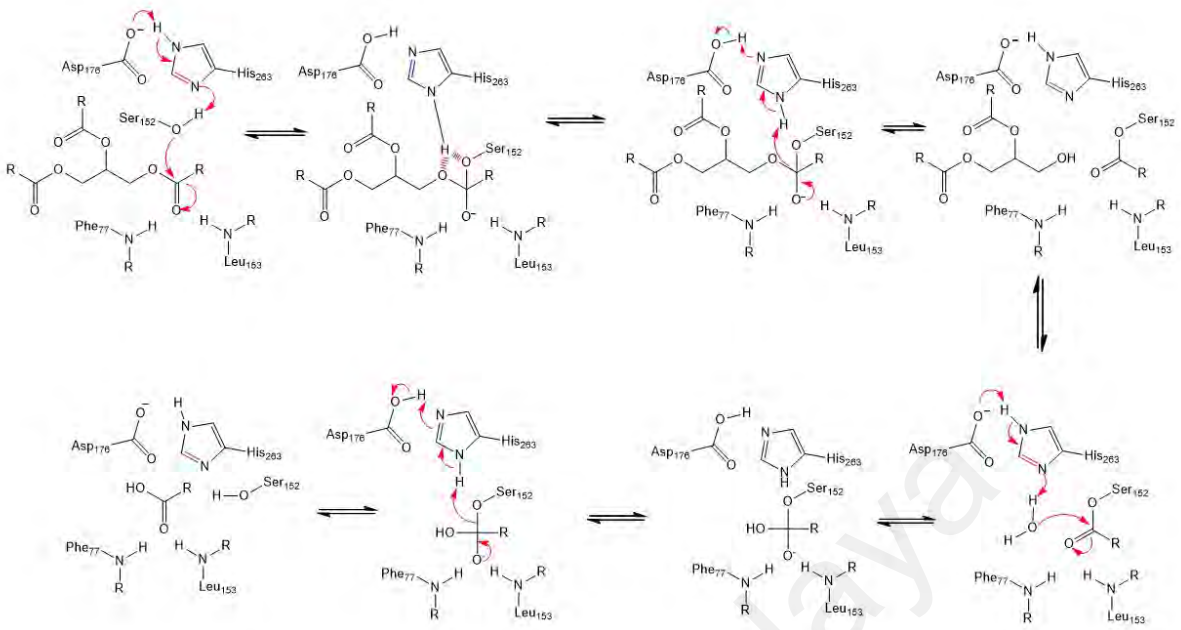

Figure 2.5. Mechanism of horse pancreatic lipase in hydrolyzing triacyglycerol (Annuar *et al.*, 2008; Gómez-Bombarelli *et al.*, 2013a)

2.6 DEGRADATION OF PCL

Degrading the long PCL chain into moderate length makes the blending process among polymers more amenable to control variables. Degradation is defined as scission of main-chain bonds producing shorter oligomers, monomers and/or other low molecular weight degradation products (Gopferich, 1996). One of the methods to modify the features of PCL is by erosion. 'Erosion' is the loss of materials i.e. monomer and oligomer groups leaving the polymer (Tamada & Langer, 1993). Surface modification or surface erosion of PCL can be employed by hydrolyzing the PCL in water to create highly porous film with a large surface to volume ratio that makes them suitable for tissue engineering applications (Ansari & Amirul, 2013). It is well known that lipase will attack at the amorphous region followed by crystalline regions. It is also conceivable that at the beginning of degradation, water molecules penetrate mostly at amorphous regions in the polyester film and act as nucleophile in the hydrolysis of ester bond (Gumel *et al.*, 2012). However, degradation at the crystalline regions may vary

from degradation at the amorphous regions because highly ordered polymer chains hinder the water penetration.

In order to understand the degradation at the crystalline regions, Iwata and Doi (2002) studied degradation of single crystal PCL as a model of the lamellar crystal region in solvent-cast and melt-crystallized films using Novozyme 435. The researchers proposed that a single crystal consists of three chain-packing states, which begin with tight chain-packing aligning perpendicular to the lamellar base, followed by tight chain-packing region with molecular chains inclining from the lamellar base and lastly loose chain-packing region. This arrangement indicates that a single crystal was made up from nano-order micro-crystals. The structural hierarchy was proposed following observation that enzyme-catalyzed degradation progresses from loosely chain-packing perpendicular to lamellar growth faces.

On the contrary, acid catalyzed degradation of PCL *via* random chain scission was observed by Kobayashi *et al.* (2000). They found that at 24 hours of reaction, intermediate molecular weight PCL is formed before gradually being reduced to oligomers at 72 hours. However, in organic solvent the chain scission is quite specific as reported by Matsumura *et al.* (2000) and Kobayashi *et al.* (2000). No formation of intermediate molecular weight was observed other than cyclic dimer and oligomers. Kondo *et al.* (2002) proposed that cyclic dimer was formed due to back-biting mechanism. Therefore, an understanding of the mechanism involved in the enzymatic degradation processes would allow us to exert some control on the production of PCL oligomers.

2.7 WATER ACTIVITY (a_w)

Thermodynamic equilibrium in reaction catalyzed by hydrolase can be shifted in the opposite direction by changing the water content in the reaction medium. High amount of water in reaction medium results in hydrolysis reaction while low concentration of water favor a synthesis reaction (Lo *et al.*, 2010). To study the water effects in organic media, the amount of water present in the reaction mixture is preferably expressed in terms of its thermodynamic activity (a_w) instead water content or water concentration. Thermodynamic water activity describes the distribution of water between the various phases that can compete in binding water (Halling, 1994).

According Engelberg and Kohn (1991), the highest hydrolytic activity rates for Novozyme 435 were obtained at higher a_w (a_w = 0.84) in toluene and carbon tetrachloride while highest transesterification activity were observed at lowest a_w (a_w < 0.1). However, total activity of lipase was decreased when a_w was increased in polar solvent (1,4-dioxane). This could be explained by enzyme denaturation due to cooperative effect between water and the polar solvent (Yang *et al.*, 2002). In enzyme recycling, the activity decreased to 40 % of the initial value at second reaction cycle and remained constant for the third- and fourth cycles. This behavior can be ascribed to either partial enzyme denaturation or dissociation of the immobilized enzyme complex. Interestingly, enzyme activity was partially recovered up to 60 % after dissolution in buffer and lyophilizing it again, suggesting that this process helps to restore at least in part of enzyme's active conformation (Secundo *et al.*, 2001)

2.8 ACTIVATION ENERGY (E_a)

The effects of temperature and activation energy on the rate of enzyme-catalyzed reaction is described by the Arrhenius equation

$$\ln k' = -\frac{E_a}{RT} + \ln A \tag{2.8}$$

where E_a is the activation energy, A is the frequency factor, R is the universal gas constant (8.3145 J mol^{-1} K^{-1}), and T is the absolute temperature (K).

In the chemical reaction, rate increases with temperature. This applies equally for enzyme-catalyzed reactions. While the initial rate of reaction increases with temperature change, the rate of reaction decreases as soon as the enzyme is thermally affected and its three dimensional conformation is altered leading to loss of enzymatic activity and possibly enzyme denaturation (Halling, 2000).

In enzyme catalyzed reactions, the values for E_a mostly range from 25 to 92 kJ mol^{-1}, while that of enzyme denaturation falls between 209 to 628 kJ mol^{-1} (Dixon & Webb, 1979). E_a for polymerization of PCL was calculated using published data of Kumar and Gross (2000) at 81 kJ mol^{-1}. These results were in agreement with the theory that the formation of ester bond requires higher energy input compared to its breakage. However, higher E_a at 200 kJ mol^{-1} was calculated for PCL solid film degradation (Marten *et al.*, 2003). Degradation of solid film by lipase is a slow process and involves complex processes starting with water molecules penetrating the amorphous region within the film, which subsequently triggers the enzyme-catalyzed hydrolysis of the ester bond and liberation of products into the medium (Wang *et al.*, 2004).

CHAPTER 3

MATERIALS AND METHODS

3.1 MATERIALS

Poly-ε-caprolactone (PCL) with average number molecular weight (M_n) 10,000 (Sigma-Aldrich; 704105), *Candida antarctica* lipase B (CALB) immobilized on acrylic resin beads (Sigma-Aldrich; L4777), toluene (Merck; 108325), 6-hydroxyhexanoic acid (Alfa Aesar; 808255), ε-caprolactone (Merck; 802801), tetrahydrofuran (Merck; 109731), were used in the study. All reagents were of analytical grade.

3.2 METHODS

3.2.1 Enzymatic degradation

PCL in the form of crystal flakes with 62.8 % degree of crystallinity (0.1 g) was dissolved in 10.0 ml of toluene, and to this solution, 100 mg of immobilized lipase B (Sigma-Aldrich; 0.01 ± 1 % U mg^{-1}) with average size of 422 ± 176 μm and average weight of 68 ± 22 μg was added into vials, with the opening crimped to provide airtight seal. The reaction was then allowed to progress for a total period 36 hours at 50 °C, 200 rpm (LabTech, Korea). In order to terminate the reaction, 3.0 ml of isopropanol was added. Then, the immobilized enzyme was filtered, and the reaction medium was dried. All reactions were performed in triplicate.

3.2.2 Product identification

The products liberated were re-dissolved in dichloromethane before injection into gas chromatography-mass spectrometry (GCMS) machine *viz.* Shimadzu GC (model 2010) coupled to Shimadzu QP 2010 Ultra MS operated in electron impact

ionization mode (70 eV) with Restek RTX-5 column (30 m long × 0.25 mm internal diameter × 0.25 μm film thickness). 1 μl of sample were injected into the GCMS using splitless mode. The inlet temperature was 200 °C. The column oven temperature profile was pre-set as follows: 90 °C for 0 min then ramped up to 280 °C at a rate of 5 °C min^{-1} and held for 10 min. Helium was used as carrier gas at a flow rate of 1.5 ml min^{-1}. For product identification, ions detected in the form of relative abundance spectra as a function of the mass-to-charge ratio (*m/z*) obtained from *GCMSsolution* software were correlated with known masses provided in the databases or their fragmentation patterns (Figure SS1 and SS2).

3.2.3 Water activity (a_w) measurement

Initial water activity (a_W) of air and toluene was recorded using Rotronic hygropalm water activity meter (HP23-AW; www.rotronic.co.uk). 10 μl of toluene was placed on the glass slide inside a sample holder. Then, a sealed container was formed by placing the probe on top of the sample holder. AwQuick mode was used to calculate the water activity and the measurement was taken after the temperature conditions were stable (both at the product and probe), usually 5 to 6 minutes after loading the sample.

3.2.4 Gel Permeation Chromatography

GPC analysis was carried out on Agilent LC 1220 (Agilent, USA) instrument equipped with a refractive index detector (Model 1260). The machine was equipped with Mixed-D gel column (7.8 mm internal diameter × 300 mm) connected to MiniMix-D gel column (5 mm internal diameter × 25 mm). The GPC measurements were used to characterize the average weight molecular weight (M_w), number average molecular weight (M_n), and the polydispersity index (PDI) of polymer fragments hydrolyzed by lipase action. Monodisperse polystyrene standards of different molecular weights (162,

380, 1020, 1320, 2930, 6770, 13030, 29150, 51150, 113300, 215000, and 483400 g mol^{-1}) (EasiVials, Agilent) were used to generate the calibration curve. The initial M_n and PDI for PCL obtained from the calibration curve was 17340 g mol^{-1} and 1.55, respectively. The polymer samples were dissolved in tetrahydrofuran (THF) at a concentration of 1.0 mg ml^{-1}, filtered through 0.22 μm PTFE filter and subsequently injected (100 μl) at 35 °C. THF at a flow rate of 0.5 ml min^{-1} was used as the mobile phase. The PDI was calculated as follows:

$$PDI = \frac{M_w}{M_n} \tag{3.1}$$

where the designated molecular weights were determined from calibration using linear polystyrene standards.

For this study, it is preferable to convert the determined M_n based on polystyrene standards to the corresponding value for PCL itself. This was firstly done for the M_n of neat PCL stock, where its initial molecular weight was calculated, following GPC analysis, using the conversion equation shown below (Chung *et al.*, 2012; Hoskins & Grayson, 2009):

$$M_n\,(\mathrm{PCL}) = 0.259 \times M_n(\mathrm{PS})^{1.073} \tag{3.2}$$

The initial M_n for neat PCL was determined at 9157 g mol^{-1}, which closely agreed with the information stated by the supplier at ~ 10 000 g mol^{-1}.

Intrinsic viscosities of PCL, [ŋ] in organic solvents were determined using Mark-Houwink-Sakurada (MHS) relation with M_w obtained *via* GPC-MALLS system (Malvern, UK). The system was equipped with a Viscotek GPCmax solvent/sample module, a Viscotek GPC column oven, a Viscotek TDA 305 triple array detector. Initial polymer samples were dissolved in THF to obtain a concentration of 5 mg mL^{-1}. Chromatography was performed at 30 °C, using a 300 × 7.8 mm TSK-Gel GMH HR-H

(TOSOH) column. Polystyrene was used as the calibration standard using THF as mobile phase at 1 mL min^{-1} flow rate. M_w value obtained was 9117 g mol^{-1} and [ŋ] in different organic solvents was obtained using MHS relations as shown below:-

PCL in Tetrahydrofuran at 30 °C, $[\eta] = 4.385 \times 10^{-4} M_w^{0.692}$ (3.3)

PCL in Benzene at 30 °C, $[\eta] = 1.96 \times 10^{-4} M_w^{0.76}$ (Mochizuki *et al.*, 1995) (3.4)

PCL in chloroform at 30 °C, $[\eta] = 1.298 \times 10^{-4} M_w^{0.828}$ (Sun *et al.*, 2006) (3.5)

In general, intrinsic viscosities of PCL at M_w = 9117 g mol^{-1} in organic solvents spanned the range of $0.2003 < [\eta] < 0.2466$.

3.2.5 Thermogravimetric analysis (TGA)

TGA analysis was conducted to measure the decomposition temperature of degradation products. The analysis was carried out on a Perkin Elmer STA 6000 (Perkin Elmer) machine. 8 to 10 mg of the sample was loaded onto the ceramic crucible pan, which was pre-flamed. The sample was heated from 30°C to 800 °C under a nitrogen flow rate of 20 ml min^{-1} at a constant heating rate of 10 °C min^{-1}. Weight loss detected below 150 ºC was neglected due to moisture content present in the sample.

3.2.6 Differential Scanning Calorimetry (DSC)

The Perkin Elmer DSC 8000 machine from Perkin Elmer was used to analyze thermal transitions of the samples. Initially, the sample was loaded onto an aluminum pan and cooled down to -60 °C to allow for completion of the crystallization. Then, the sample was heated to 300 °C at a constant rate of 10 °C min^{-1} to determine the melting curve. In order to confirm the composition of the second peak, the polymer sample was heated in nitrogen atmosphere from -60 to 300 °C, then cooled before reheating it again

for the second time. The relative crystallinity of the polymer was calculated according to the following equation:

$$DG = \frac{\Delta H_f}{\Delta H_f^0} \times 100 \tag{3.6}$$

where DG is the degree of crystallinity, ΔH_f is the heat fusion of the polymer, and ΔH_f^0 is the heat of fusion for 100 % crystalline PCL i.e. 142 J g^{-1} (Elzein *et al.*, 2004).

3.2.7 Scission models proposed by Joshi and Madras (2008)

There are two types of scission models of PCL studied by Joshi and Madras (2008) *viz*. random chain scission and chain end scission. A polymer can be expressed as a molecule having molecular weight x as a continuous variable, while $P(x)$ represents a polymer population molecular weight. In order to study CALB scission mechanism towards PCL, M_n of PCL was measured every 3 hours during reaction period and applied in equations (4.4) and (5.4). Model with good fit was selected based on the correlation coefficient R^2 and adjusted R^2 values close to 1.

3.2.7.1 Random chain scission

$$P(x) \xrightarrow{K_d(x)} P(x') + P(x - x') \tag{3.7}$$

where $K_d(x)$ represents the overall degradation rate coefficient. The time dependent molecular weight distribution of polymer P(x) is represented as $p(x,t)$. The population balance equation for degradation can be written as follows:

$$\frac{\partial p(x,t)}{\partial t} = -K_d(x) \cdot p(x,t) + 2\int_x^\infty K_d(x') \cdot p(x',t) \cdot \Omega(x,x')dx' \tag{3.8}$$

The stoichiometric kernel $\Omega(x, x')$ in Eq. (3.8) determines the distribution of scission products. For random chain scission, the distribution of degraded products, $\Omega(x, x')$ is $1/x'$. Assuming a linear dependence of K_d on x, $K_d(x) = k_d \cdot x$, the above equation reduces to

$$\frac{\partial p(x,t)}{\partial t} = -k_d \cdot x \cdot p(x,t) - 2\int_x^\infty k_d \cdot p(x',t)dx' \tag{3.9}$$

Applying the moment operation, $p^{(j)}(t) = \int_x^\infty p(x,t) \cdot x^j dx$ to Eq. (3.9) yields

$$\frac{dp^{(j)}}{dt} = \left[-\frac{j-1}{j+1}\right] \cdot k_d \cdot p^{(j+1)}(t) \tag{4.0}$$

j = 0, 1 and 2 corresponds to the zeroth, first and second moments, respectively.

$$\frac{dp^{(0)}}{dt} = k_d \cdot p^{(1)}(t) \tag{4.1}$$

$$\frac{dp^{(0)}}{dt} = 0 \tag{4.2}$$

$p^{(0)}$ and $p^{(1)}$ represent the molar concentration and mass concentration of the polymer, respectively. According to the first moment (Eq. 4.2), the mass concentration of the polymer is constant throughout the reaction. Solving eq. (4.1) with initial condition $p^{(1)} = p_0^{(1)}(t = 0)$

$$p^{(0)}(t) - p_0^{(0)} = k_d \cdot p_0^{(1)} t \tag{4.3}$$

By defining the number average molecular weight M_n, as $p^{(1)}/p^{(0)}$, Eq. (4.3) can be rearranged as

$$\left(\frac{M_{n0}}{M_n}\right) - 1 = k_d \cdot M_{n0} t \tag{4.4}$$

Eq. (4.4) showed that variation of $\left(\frac{M_{n0}}{M_n}\right) - 1$ with time is linear with the slope of $k_d \cdot M_{n0}$

3.2.7.2 Chain end scission

The fragmentation reaction, which yields a molecule of specific molecular weight of products, can be written in continuous distribution model approach as follows:

$$P(x) \xrightarrow{k_s(x)} Q(x_s) + P(x - x_s) \tag{4.5}$$

where $k_s(x)$ represents the degradation rate coefficient. The instantaneous concentration of species P and Q is $p(x,t)$ and $q(x,t)$ respectively. The population balance equations are

$$\frac{\partial p(x,t)}{\partial t} = -k_s \cdot p(x,t) + k_s \int_x^\infty p(x',t) \cdot \delta(x(x - x_s))dx' \tag{4.6}$$

$$\frac{\partial q(x,t)}{\partial t} = -k_s \cdot p(x',t) \cdot \delta(x_s, x')dx' \tag{4.7}$$

For chain end scission, we assume k_s to be independent of x. Applying moments on Eq. (4.6).

$$\frac{dp^{(j)}(t)}{dt} = -k_s \cdot p^{(j)}(t) + k_s \sum_{i=0}^{j} j_{C_i} (-x_s)^i \cdot p^{(j-i)}(t) \tag{4.8}$$

The zeroth and first moments are obtained by substituting j = 0 and 1, respectively, in Eq. (4.8).

$$\frac{dp^{(0)}}{dt} = 0 \tag{4.9}$$

$$\frac{dp^{(1)}}{dt} = -k_s \cdot x_s \cdot p^{(0)}(t) \tag{5.0}$$

Eq. (4.9) suggests that molar concentration remains constant during chain end scission.

$$p^{(0)}(t) = p_0^{(0)} \tag{5.1}$$

Solving eq. (20) with the initial condition that at $t = 0$, $p^{(1)} = p_0^{(1)}$

$$p^{(1)}(t) = p_0^{(1)} - k_s \cdot x_s \cdot p^{(0)}(t) \tag{5.2}$$

By defining the number average molecular weight, M_n as $p^{(1)}/p^{(0)}$. Eq. (22) can be rearranged as

$$M_n = M_{n0} - k_s \cdot x_s \cdot t \tag{5.3}$$

Eq. (23) shows that variation of M_n versus t is linear with slope $k_s \cdot x_s$. Here x_s is taken as molecular weight of monomer, 114 g/mol, determined by GC-MS as described earlier. The evolution of the monomer is following specific chain-end scission from hydroxyl end of the chain (Joshi & Madras, 2008).

3.2.8 Calculation of degree of crystallinity

To obtain a correlation between degree of crystallinity for PCL and enzymatic hydrolysis as a function of time, the following exponential decay model has been proposed and transformed from Mook Choi *et al.* (2003).

$$\frac{DG(t)}{DG(0)} = \exp\left(-\frac{t}{\sigma_s}\right) \tag{5.4}$$

where DG(t) and DG(0) are the percentage crystallinity of PCL at times t and t = 0, respectively. σ_s is an adjustable parameter and $1/\sigma_s$ is the rate of degradation.

3.2.9 Calculation of activation energy, E_a

Activation energy was calculated using linearized Arrhenius relationship as mentioned previously (Eq. 2.8):

$$\ln k' = -\frac{E_a}{RT} + \ln A \tag{2.8}$$

where E_a is the activation energy, A is the frequency factor, R is the universal gas constant (8.3145 J mol^{-1} K^{-1}), and T is the absolute temperature (K). In order to calculate rate constant, k', the initial rate of dicaprolactone (DCL) production was plotted against different PCL concentrations for each tested temperature (30 to 50 °C).

The k' value was obtained from the slope of the linear plot. Subsequently, graph ln k' versus 1/T was constructed, and activation energy of degradation was calculated by multiplying the slope of the plot with universal gas constant, *R*.

CHAPTER 4

RESULTS AND DISCUSSION

4.1 MOLECULAR WEIGHT DETERMINATION

Prior to the study of the mechanism of lipase-catalyzed hydrolysis of PCL in toluene, molecular weight changes of PCL after hydrolysis need to be measured. Reduction in initial molecular weight of PCL indicated that lipase was actively hydrolyzing the PCL chains in toluene. No hydrolysis of PCL was observed in toulene without the addition of lipase. The molecular weight profile for the degradation of PCL by lipase B from *Candida antarctica* (CALB) is shown in Figure 4.1. PCL in toluene without the addition of CALB (control) showed a single peak (*A*) indicating that PCL is neither self-hydrolyzed in toluene nor the solvent itself could catalyze the hydrolysis of PCL. When lipase was included in the reaction mixture, the peak area of PCL was observed to be decreasing with time, showing that lipase successfully hydrolyzed the PCL in toluene. The subsequent peak (*B*) was detected at almost identical retention time, after three hours reaction, corresponding to the remaining high molecular weight chain of bulk PCL following lipase degradation (Figure 4.1). In the same chromatogram (*B*), smaller molecular weight fragments or oligomers arising from PCL hydrolysis were eluted at later times. Within three hours of hydrolysis, the bulk polymer M_n declined significantly alongside the liberation of fragments with smaller molecular weights. The refractive index of peaks eluted at later times (*C, D* and *E*), corresponding to these fragments, increased with reaction time indicating that the concentration of fragments from hydrolysis reaction also increased (Figure 4.1).

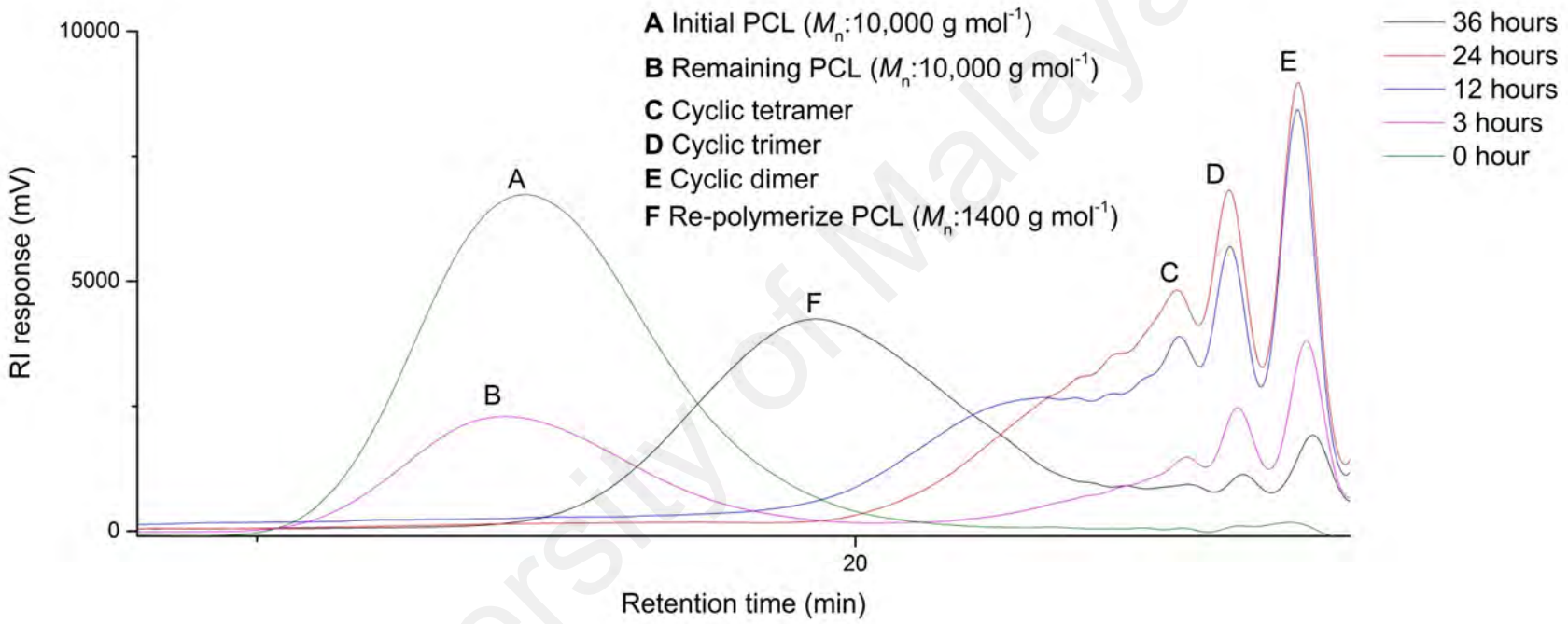

Figure 4.1. GPC chromatogram of molecular weight distribution for lipase-mediated hydrolysis of PCL in toluene at 50 ºC.

After 24 hours of reaction, molecular weight analysis based on polystyrene standards showed the presence of three major fractions *viz.* M_n : 293 g mol^{-1}, M_n : 434 g mol^{-1} and M_n : 843 g mol^{-1} while the initial bulk PCL peak (*A*) had disappeared showing that PCL was almost entirely hydrolyzed by lipase. The M_ns were converted using equation (3.2) to obtain the corresponding M_ns for fragments from PCL hydrolysis i.e. 114 g mol^{-1}, 175 g mol^{-1} and 353 g mol^{-1} respectively.

From GCMS analysis, the degradation products were identified as cyclic dimer (M^+ : *m/z* 229.05) for peak *E*, cyclic trimer (M^+ : *m/z* 344.15) for peak *D*, and cyclic tetramer (M^+ : *m/z* 457.25) for peak *C*. Kobayashi *et al.* (2000), Ebata *et al.* (2000) and Kondo *et al.* (2002) identified the presence of cyclic oligomers when using immobilized *Candida antarctica* lipase (CAL) for PCL hydrolysis in toluene and supercritical carbon dioxide. The high abundance of mass-to-charge (*m/z*) ratios of 69, 97, and 115 ions corresponding to each *C, D* and *E* peaks indicated cyclic lactone formation in this study. The parent ions for each of the generated lactones from PCL hydrolysis were shown in Table 4.1.

Table 4.1. Relative abundance of mass-to-charge ratio of parent ions after electron impact ionization (EI).

Mass-to-charge ratio (*m/z*)	Relative abundance (%)			
	Dimer	Trimer	Tetramer	Caprolactone
55.10	100.0	81.1	55.8	26.6
69.05	68.1	56.1	33.8	1.9
96.05	42.8	28.1	11.8	0.0
97.05	91.8	74.5	32.8	0.3
114.10	39.7	24.2	9.3	9.8
115.10	100.0	100.0	100.0	0.8

It was hypothesized that the formation of dimeric, trimeric and tetrameric fragments proceeded through first tetrahedral intermediate within the active site of lipase (Figure 4.2). This generated an acyl-enzyme intermediate. In the presence of abundant water molecules, they can act as nucleophile to attack acyl-enzyme intermediate resulting in linear degradation fragments. Kondo *et al.* (2002) reported that when water concentration was increased, yield of dicaprolactone (DCL) decreased concomitantly with higher yield of linear 6-hydroxyhexanoate oligomers. Kobayashi *et al.* (2000) also investigated the lipase-catalyzed polymerization of lactones in water saturated isopropyl ether (water content of *ca.* 0.2 %), and they also found that the products were mainly linear oligomers.

However, in the isolated environment with low water content such as applied in this study (initial a_w for toulene and air in equilibrium = 0.81 ± 0.01), we proposed that ring-closing reaction through nucleophilic attack by terminal hydroxyl from hydrolyzed product itself acting as a nucleophile predominates. When mediated by lipase, it forms second tetrahedral intermediate complex and subsequently released as cyclic lactone (Figure 4.2).

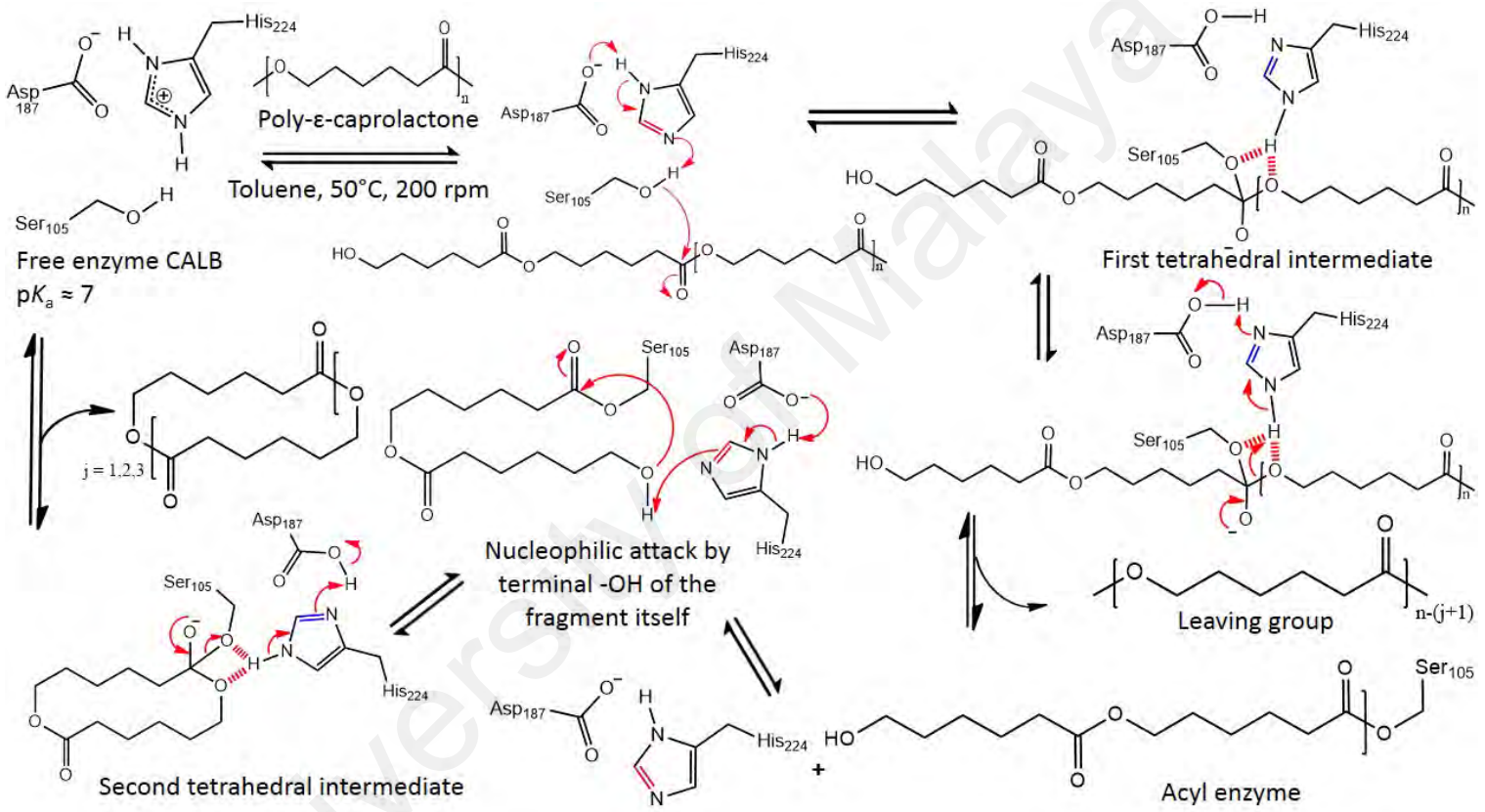

Figure 4.2. Proposed mechanism of lipase-catalyzed scission of poly-ε-caprolactone and the subsequent formation of cyclic dimer (dicaprolactone) in toluene. The steps are equally applicable for the formation of cyclic trimer and tetramer as found in this study.

This could explain the undetected linear equivalents of the cyclic dimer, trimer and tetramer fragments (Figure 4.3). Cyclic fragments longer than tetramer were not detected since it was expected that the cyclization of longer fragments would be more difficult to accomplish. In hindsight, both earlier findings by Kobayashi et al. (2000) and Kondo et al. (2002) indirectly supported the proposal that CALB was responsible for the formation of cyclic lactone in low water content environment. Our proposed route to cyclic lactone mediated by lipase action also provide possible explanation to the back-biting mechanism as proposed by Kondo et al. (2000).

At 24 hours of reaction, PCL peak diminished completely and evident presence of low molecular weight fragments of identities discussed earlier (Figure 4.1 - chromatogram *C*). Interestingly, as hydrolysis reaction was allowed to proceed to 36 hours, formation of peak *F* with indicated intermediate M_n in between the M_ns of hydrolyzed products and neat PCL (Figure 4.1). It has been reported by Gumel *et al.* (2012) that low water content and water activity of toluene resulted in the polymerization of caprolactone by lipase. During the late reaction phase, it was hypothesized that water content/activity had reduced sufficiently low to allow lipase to re-polymerize low molecular weight fragments and produced intermediate polymer with molecular weight of 1.4×10^3 g mol^{-1}. The re-polymerization was further encouraged by the low molecular weight fragments acting as nucleophile. The steep reduction in intensities of peaks *C, D* and *E*, at 36 hours (chromatogram *F*), supported the re-polymerization occurence attributed to lipase activity.

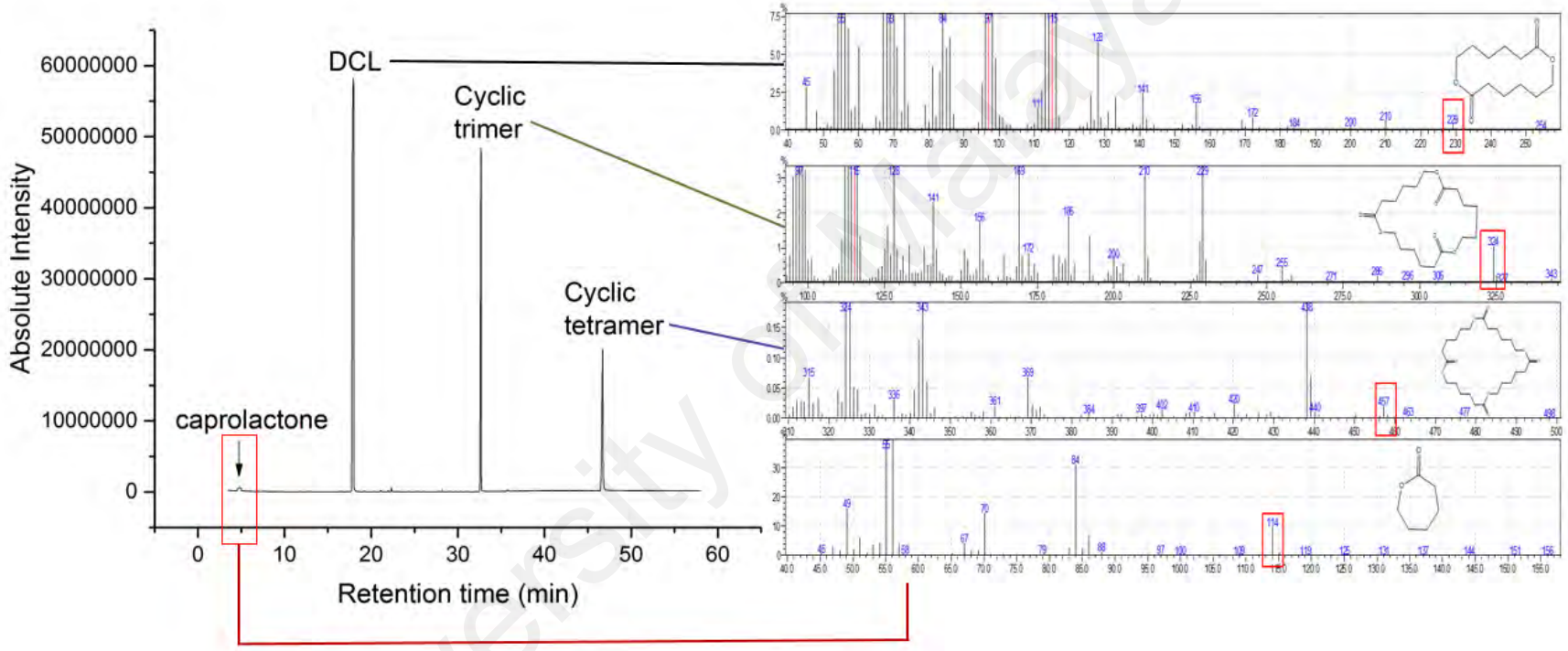

Figure 4.3. GCMS chromatogram of PCL samples after 26 hours of reaction. MS data obtained from *GCMSsolution* software showed mass-to-charge ratio of caprolactone ($M^{+\cdot}$ *m/z* 114.14) , DCL ($M^{+\cdot}$ *m/z* 229.05), cyclic trimer (M^{+} : *m/z* 344.15) and cylic tetramer (M^{+} : *m/z* 457.25).

4.2 LIPASE SCISSION MECHANISM

The plots of M_n, M_w and PDI versus reaction time were shown in Figure 4.4. Both M_n and M_w showed marked decrease with time particularly in the early part of the hydrolysis. A sharp increase in the polydispersity index (PDI) in the first 4 hours was attributed to the liberation of oligomers from PCL hydrolysis. Substantial loss of M_n and M_w from lipase attack at the polymer backbone was hypothesized, yielding DCL and oligomers with M_n less than 500. As the reaction proceeds, M_n value reached a plateau after 4 hours while M_w and PDI values gradually reduced indicating that lipase was still degrading the polymer chain until relatively low M_w and narrow PDI was obtained compared to the early phase of hydrolysis.

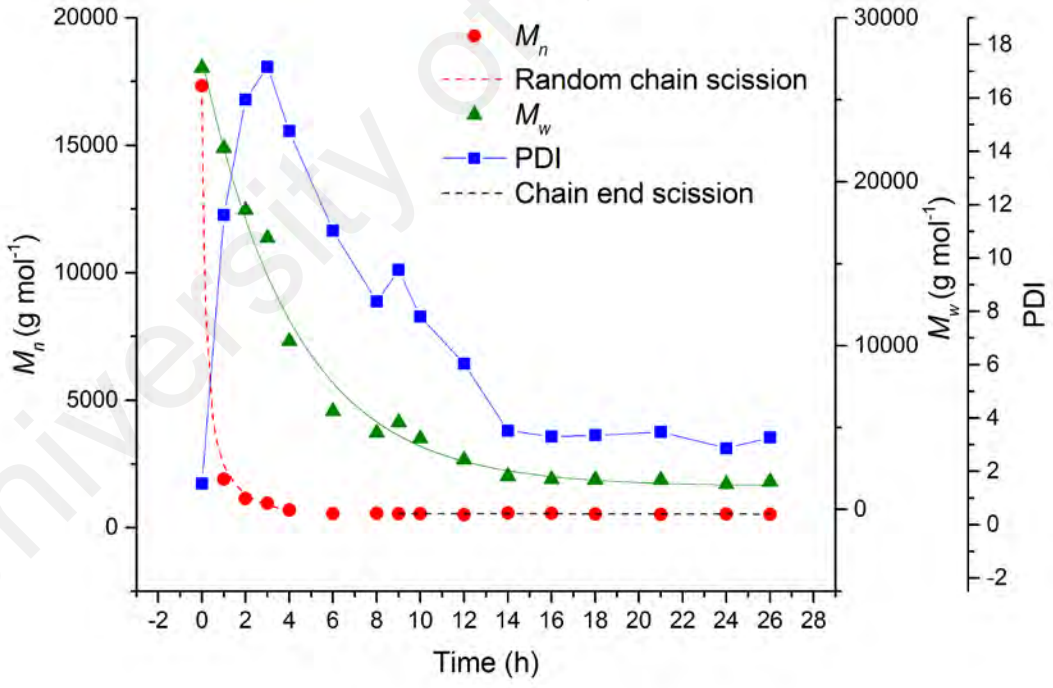

Figure 4.4. Degradation profiles of PCL for 26 hours reaction with 0.1 g of CALB at 50 °C. Unconverted M_n values were used for this profile. Red and black dash lines indicate theoretical curves for random and chain end scission models, respectively.

However, PDI value did not approached closer to 1 despite prolonged reaction time up to 26 hours. This showed that the oligomer populations produced from lipase hydrolysis of PCL was made up of heterogeneous chain length fragments. This occurrence was suggested to be due to random scission of PCL backbone, which resulted in the mass distribution pattern shown (Figure 4.4).

When variable (M_{n0}/M_n)-1 versus time was plotted according to equation (4.4), a linear relationship was obtained (Table 4.2) suggesting that hydrolysis of PCL using lipase in toluene at 50 °C proceeded by random chain scission on the polymer backbone during early phase of reaction. From the slope of the curve, the degradation rate constant, k_d was calculated to be 3.52×10^{-4} h^{-1}.

Even though the changes in M_n and M_w appeared to be almost constant after 9 hours of reaction (Figure 4.4), linear relationship was observed when variable M_n versus time (Table 4.2) was plotted according to equation (5.3). This indicated that hydrolysis of PCL by lipase occurred *via* specific chain-end scission from 9 to 26 hours. PCL fragmentation *m/z* ratio from GC-MS analysis showed the presence ε-caprolactone at 26 hours of reaction (Figure 4.3), thus supporting the specific chain-end scission hypothesis during the late phase of reaction, albeit its amount was significantly less than dimer and oligomers. The degradation rate constant during the late phase of PCL hydrolysis, k_s was calculated at 0.013 h^{-1}. The post-regression statistics for both models were shown in Table 4.2.

It was clear that random and chain end-scission models (R^2: 0.9837 and 0.9336) showed good fits to the experimental data. Both models showed relatively small root-mean-square deviation (RMSD) and variance, therefore, indicating that random and chain end-scission models proposed by Joshi and Madras (2008) were able to explain the degradation of PCL by CALB in toluene for early- and later phase of reaction,

respectively. It has been reported that mechanism of lipase degradation towards PCL occurs solely as random chain scission of the ester linkage (Kondo *et al.*, 2002; Kweon *et al.*, 2003).

Table 4.2. Value of kinetic parameters of chain scission models.

Chain scission model	Values of kinetic parameters (± 95% confidence interval)		Correlation coefficient (R^2)	R^2 adjusted	RMSD	Variance (σ)
	k_d (mol g^{-1} h^{-1})	k_s (h^{-1})				
Random chain scission $\left(\frac{M_{n0}}{M_n}\right) - 1 = k_d M_{n0} t$	3.52×10^{-4} ($\pm$ 1.25×10^{-5})	-	0.9837	0.9837	0.3920	1.4051
Chain end scission $M_n = M_{n0} - k_s x_s t$	-	0.0132 ($\pm$ 0.0016)	0.9336	0.9204	0.9407	8.6724

RMSD: root-mean-square-deviation

From the findings in this study, we presented evidence that lipase in the form of CALB hydrolyzes PCL in toluene *via* random chain scission of polymer backbone in the early phase of hydrolysis while at the later phase specific chain-end scission ensued. The random chain scission was supported by the steep decline in M_n and M_w, and sharp increase in PDI during the early phase (0 to 4 hours). On the other hand, after 9 hours of reactions, very little changes were observed for M_n and M_w; while PDI remain constant (~ 3) during the late phase of reaction (14 to 26 hours) indicating that random chain scission was no longer the pre-dominant mechanism. Instead, the presence of monomer ε-caprolactone among hydrolysis products indicated that the specific chain-end scission of polymer fragments also occurred. It is suggested that the likeliness of ε-caprolactone monomer being generated from the hydrolysis of cyclic oligomers (dimer, trimer, tetramer) was small compared to chain-stretched PCL. For instance, hydrolysis of mevalonolactones is non-spontaneous due to negative entropy changes ($\Delta S < 0$) and

higher overall free energy changes (ΔG) for hydrolysis at 3.82 kcal mol^{-1} in HCL/KCL buffer (Kaufman, 1990). In addition, Gómez-Bombarelli *et al.* (2013b) reported that medium-sized or large lactones do not hydrolyze in neutral medium.

4.3 TRANSFORMATION OF PCL INTO CYCLIC OLIGOMERS AND THERMAL CHARACTERIZATION

Figure 4.5 showed thermogravimetric (TG) curves for degradation of PCL at different reaction times. The shapes of PCL weight loss curves were altered at different reaction times while the temperature for the maximum oxidation (T_{max}) showed a slight decrease as reaction time increased especially for tetracaprolactone fraction (Table 4.3). The observation was attributed to irregular shape of tetracaprolactone fraction peak at 12 hours resulting in a deviation for T_{max} calculation (Figure 4.5).

The weight loss pattern for pure PCL was a single-step decomposition process and can be observed by the presence of a single derivative TG (DTG) peak at 408 °C in Figure 4.6. However, this was not the case for the rest of samples from the reaction mixture (t = 1, 3, 6, 9, 12 hours). It was clear that weight losses of the heated samples occurred in several steps (Figure 4.6), indicating a mixture of masses with varying thermal properties. The maximum oxidation temperatures obtained from DTG curves were summarized in Table 4.3.

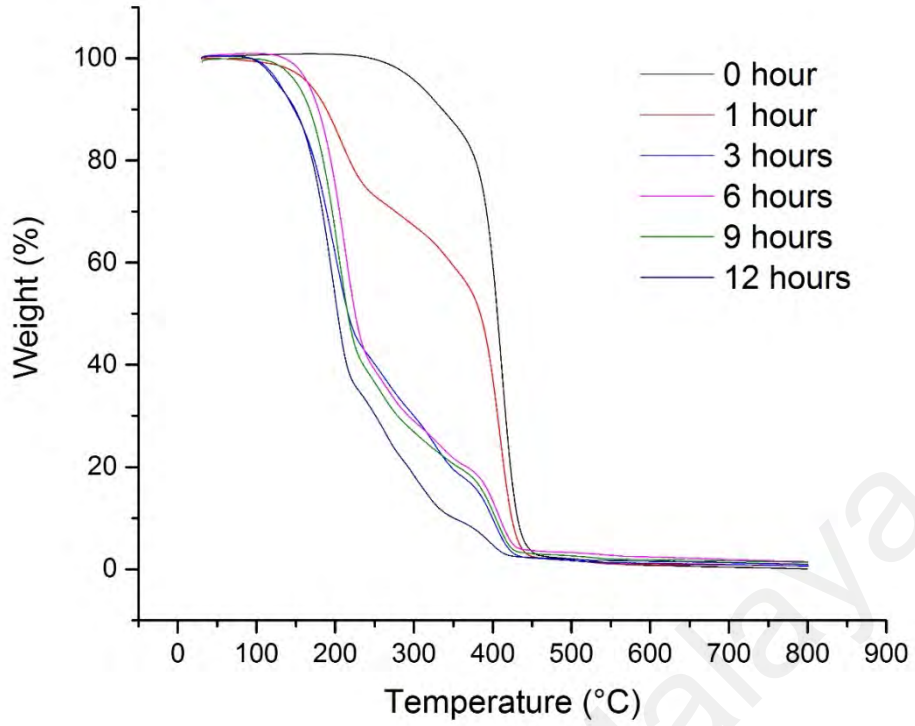

Figure 4.5. Weight loss profile of PCL at various reaction times (t = 0, 1, 3, 6, 9 and 12 hours).

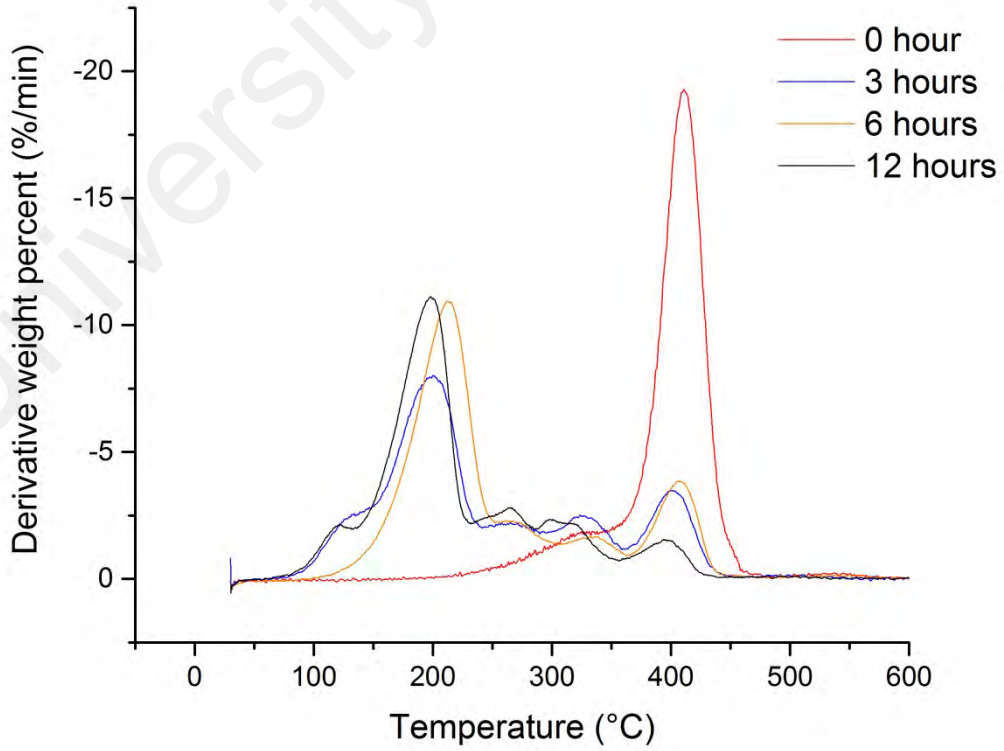

Figure 4.6. Derivative thermogram (DTG) of lipase-hydrolyzed PCL at different reaction times

Table 4.3. Maximum decomposition temperature of dicaprolactone, tricaprolactone, tetracaprolactone and PCL

Time (h)	T_{max} (°C)			
	DCL	Tricaprolactone	Tetracaprolactone	PCL
0	n.d	n.d.	n.d.	408
1	208	n.d.	342	409
3	200	271	327	402
6	213	270	336	407
9	205	260	n.d.	402
12	198	265	300	396

n.d. : not detected

Four overlapping peaks can be observed from the DTG curves in Figure 4.6. The peaks corresponding to dicaprolactone (200 - 212 °C), followed by tricaprolactone (260 - 270 °C), tetracaprolactone (300 - 342 °C) and lastly, PCL (396 - 408 °C). At 1 and 9 hours of reaction time, tricaprolactone and tetracaprolactone peaks were completely overlapped due to both fragments having almost similar rate of decomposition, therefore it was difficult to distinguish the exact maximum decomposition temperature (T_{max}). Both TG and GPC data corroborated the earlier suggestion that PCL was almost entirely degraded by lipase into dicaprolactone, tricaprolactone and tetracaprolactone.

Figure 4.7 showed the profile of weight loss of PCL and accumulation of dicaprolactone within 12 hours of degradation by CALB. Percentage weight losses of PCL and dicaprolactone yield were obtained by integrating area under the curve of DTG chromatograms. Both profiles showed rapid increase at the beginning of reaction before reaching plateau after 6 hours. Maximum weight loss of PCL was observed at 92 % and the highest dicaprolactone production was 67 %. Rate constant for dicaprolactone production was calculated at 0.64 h^{-1}, slower than rate constant for PCL hydrolysis at 0.77 h^{-1}. Thus, CALB catalysis required only about an hour to reduce more than half of the total weight of PCL into dicaprolactone and oligomers. These results also translated

into almost 75 % of degraded PCL were converted into dicaprolactone and the remaining 25 % was hydrolyzed into a mixture of tricaprolactone and tetracaprolactone.

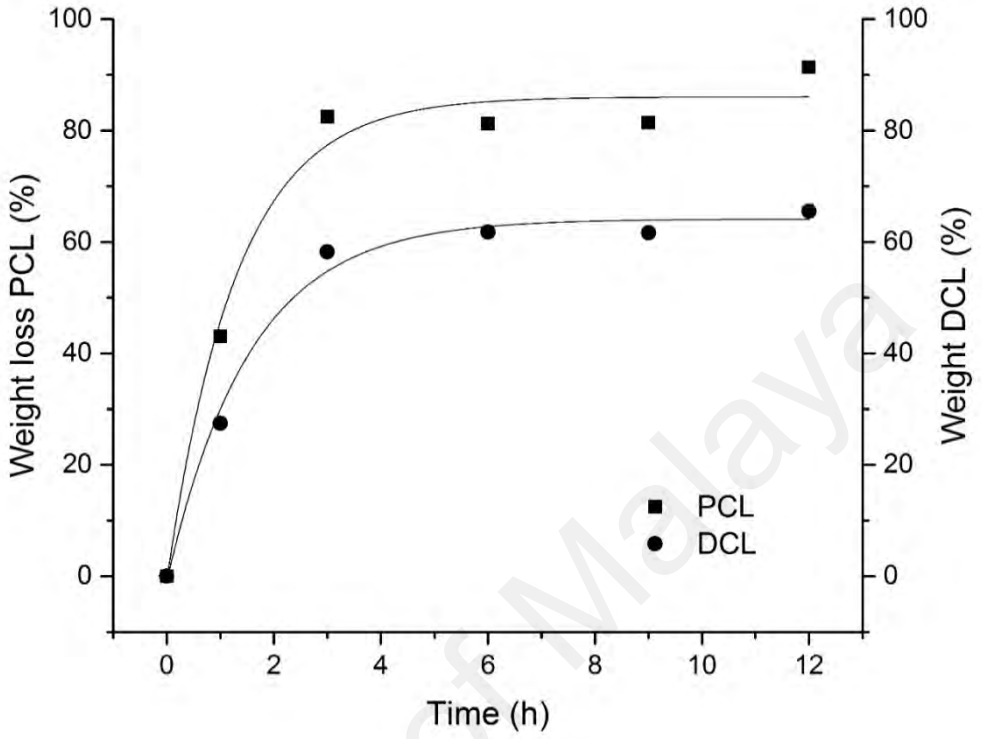

Figure 4.7. Changes in weight loss of PCL and weight gain by monomer during 12 hours of reaction as determined by thermogravimetric analysis (TGA).

Differential scanning calorimetry (DSC) was further used to characterize the products of PCL hydrolysis by lipase. Thermogram of the PCL samples was shown in Figure 4.8. The degraded polymer samples showed lower melting points (T_m) and enthalpy (J g^{-1}) than initial neat PCL as a function of reaction time (Table 4.4). Jenkins and Harrison (2008) reported that the melting point of polymer is proportional to the lamella thickness of the melting crystal.

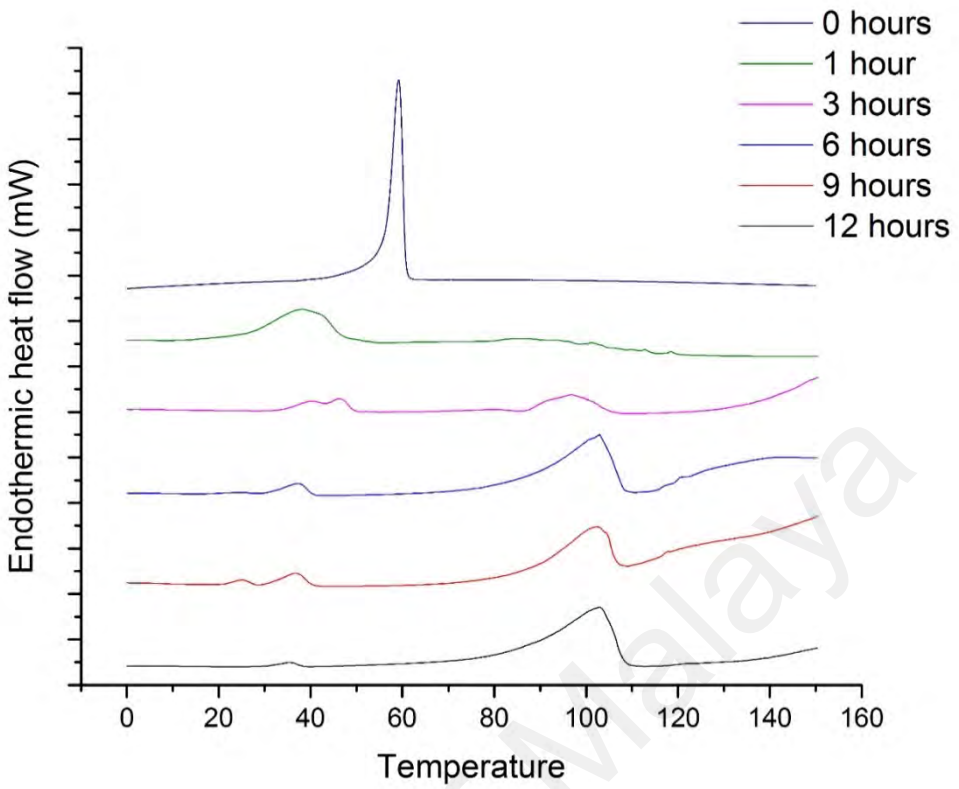

Figure 4.8. Profile of melting point for degraded PCL (T_m) from differential scanning calorimetry at heating rate of 10 °C min^{-1}.

Table 4.4. Melting point of PCL and enthalpy of heating for different reaction times

Time (h)	T_m (°C)	Enthalpy (J g^{-1})
0	59.20	89.22
1	38.53	38.41
3	46.52	9.76
6	37.53	4.73
9	37.05	5.80
12	35.00	1.65

The occurrence of two peaks in Figure 4.9, one with low melting point at 50°C corresponding to residual thin lamellae after hydrolysis, while the high melting temperature peak at 103 °C starting from 3 hours of reaction time corresponded to formation of highly crystallized structure among the hydrolyzed products. Sammon *et al.* (2000) attributed this to the so-called 'chemicrystallisation' process where shorter chain segments with enough mobility tend to realign and crystallize. As reaction

progressed, continuous hydrolysis of PCL by CALB generated high concentration of short chain fragments that realigned and continuously being loaded among themselves to form thicker crystalline lamellar stacks than before the degradation process. During the first heating, two peaks were observed at 35 °C and 102.93 °C, while after the second heating process, only a single peak was observed at 49.99 °C. The loss of peak at 102.93 °C was attributed to the decomposition of dicaprolactone (T_d : 203 ± 10 °C), tricaprolactone (T_d : 268 ± 13 °C) and tetracaprolactone (321 ± 16 °C). The DSC data pointed to the possibility of 'chemicrystallization' of small molecular weight fragments from hydrolysis of PCL.

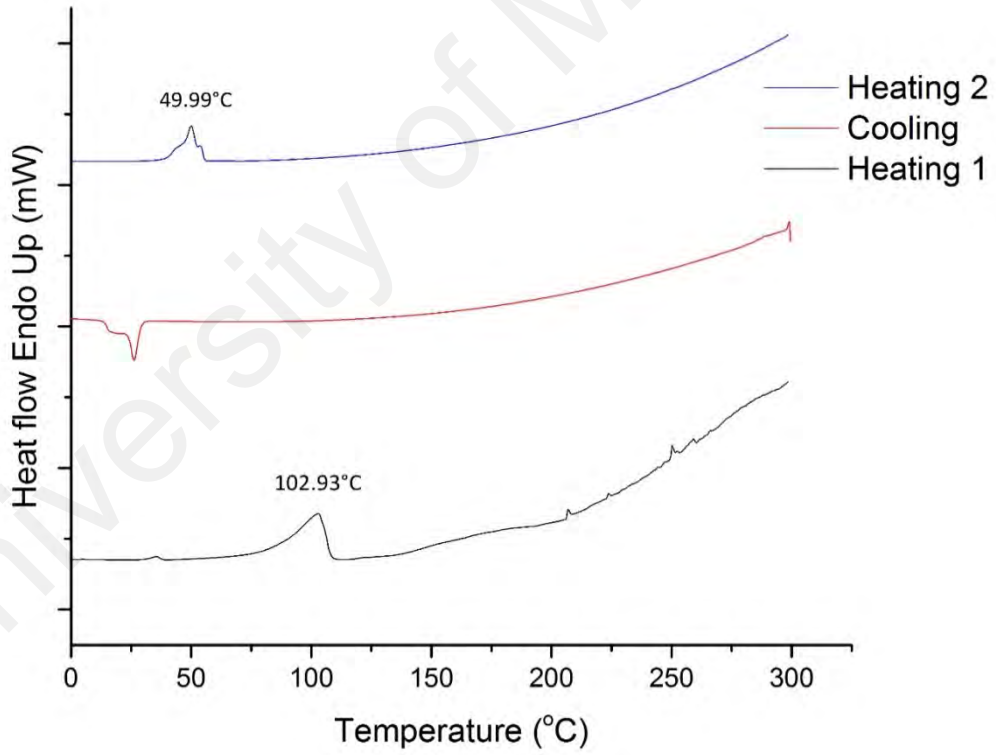

Figure 4.9. Thermogram of PCL after 12 hours of reaction. Reaction conditions: 0.01 g PCL, 0.1 g CALB, 50 °C and 200 rpm.

The initial rapid descend in M_n, crystallinity and weight percentage of PCL can be attributed to relatively high probability of available, active enzyme supplied in the reaction mixture participating in successful hydrolyses of PCL backbone immediately at

the start of reaction (Figure 4.10). However, after 2 hours and high concentration of degradation fragments being generated, rate of reduction of M_n, crystallinity and weight percentage of PCL became near constant (Figure 4.10). This was in contrast to aqueous degradation of PCL film where reduction in weight loss and increase in degree of crystallinity was observed as initial degradation proceeds rapidly at the amorphous region compared to the subsequent hydrolysis of the crystalline region (Jenkins & Harrison, 2008). In addition, Iwata and Doi (2002) reported that degradation of the PCL single crystal in phosphate buffer generated water soluble monomer and dimer of PCL but then the molecular weight of the crystals remained relatively unchanged. This indicated that partial degradation at the chain-folding surfaces was lacking (Iwata & Doi, 2002).

The first 3 hours of reaction showed a fast decrease in degree of crystallinity before reaching a plateau between 6 and 12 hours (Figure 4.10). The initial degree of crystallinity of PCL in toluene was calculated at 62.8 % before massively decreased to 1.3 % at a rate constant of 0.87 h^{-1} within 12 hours of reactions. Reduction in crystallinity was observed previously when PCL film was degraded in phosphate buffer solution by lipase (Gan *et al.*, 1997; Gan *et al.*, 1999; Iwata & Doi, 2002).

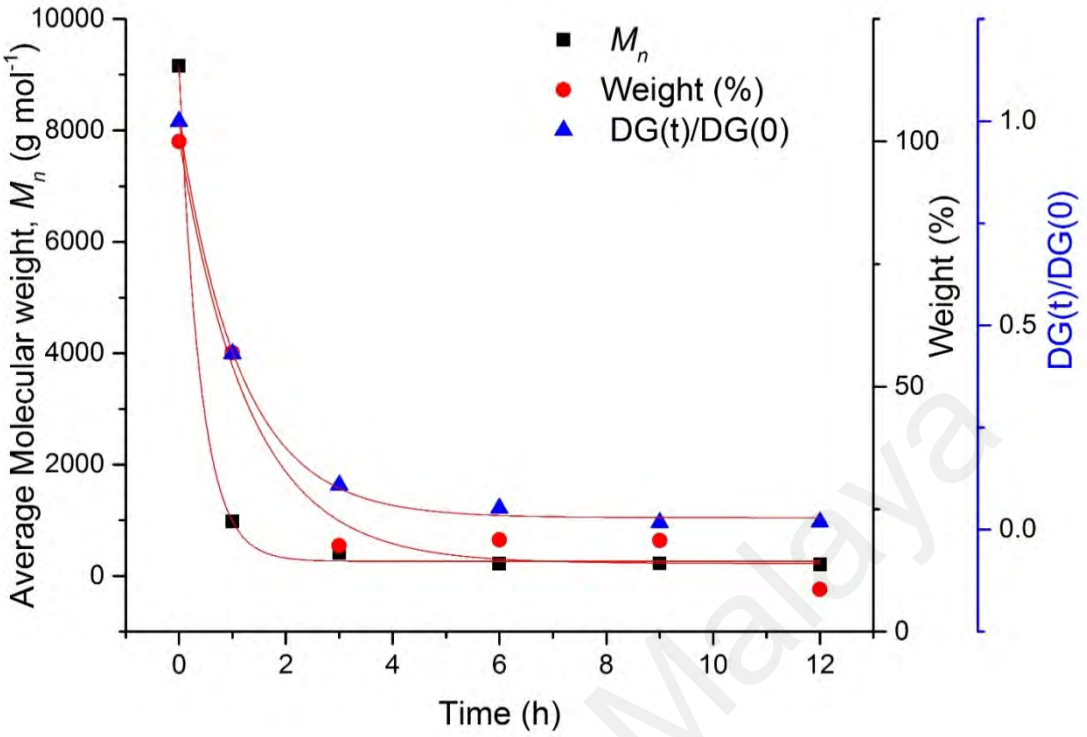

Figure 4.10. Profiles of M_n, weight percentage of PCL (%), and degree of crystallinity during 12 hours reaction.

The observation made was explained as the following: when the polymers were dissolved in a solvent, the solvent molecules diffuse through the polymer matrix until they reached the polymer core and stretched the polymer backbone to form a swollen, solvated mass (Figure 4.11). Then, it broke up and the polymer chains started to disperse into true solution (Huang, 1995; Stevens, 2009). Natural structure of polymer chains in solution can be expressed based on α value obtained from Mark-Houwink-Sakurada relation (MHS). For random coiled polymer in theta solvent, α value varies between 0.5 and 0.8, and for more rodlike extended-chain polymer, α value may be as high as 1.0 (Stevens, 2009). Since α value of PCL in organic solvent range between 0.69 - 0.82 (Eqs. 3.3 – 3.5), PCL chains disperse as flexible random coiled. It is well known that lipase preferred to cleave bond at the amorphous regions compared to crystalline region due to the tight arrangement at the crystalline regions. Once the

polymer dissolve in an organic solvent, both regions turns into flexible random coil chain making the ester bond, neither in amorphous regions nor in crystalline regions, prone to be cleaved by CALB as shown in Figure 4.11. Dispersion of the polymer matrix allowed the CALB beads with average size of 422 ± 176 μm to further penetrate the PCL backbone and catalyzed scission. In contrast to PCL crystal degradation in aqueous solution as reported by Iwata and Doi (2002), substantial reduction in the degree of crystallinity alongside M_n was observed for PCL following enzymatic hydrolysis in solvent.

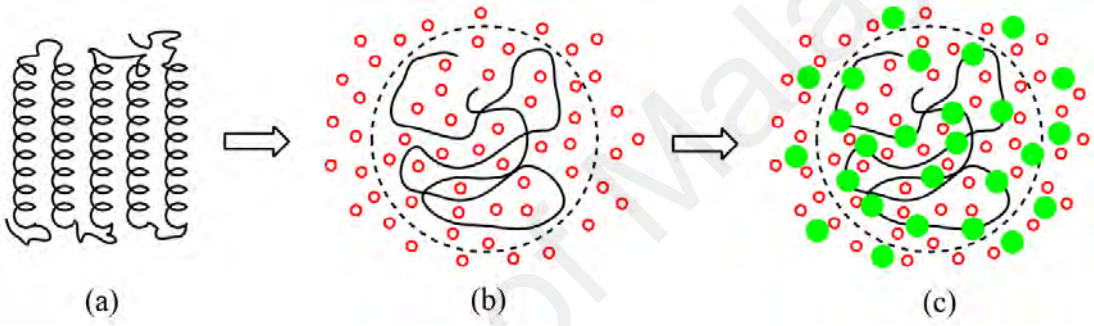

Figure 4.11. Schematic diagram of poly-ε-caprolactone (PCL) molecule. (a) Semi-crystalline structure (b) Solvated polymer molecules dispersed in toluene as flexible random coil chain, α = 0.69 - 0.82 (c) Immobilized CALB randomly attached to the polymer chains. The red circles represent toluene molecules, and solid green circles represent immobilized CALB (*not to scale*). In dilute solution, strong polymer-polymer interactions are replaced by the weaker polymer-solvent interactions.

4.4 EFFECTS OF PCL CONCENTRATION AND TEMPERATURE ON LIPASE HYDROLYSIS ACTIVITY

PCL concentration in toluene can be expected to be one of the critical factors affecting efficiency of lipase hydrolysis. Figure 4.12 showed the relationship between the initial rates of degradation as a function of PCL concentration and temperature for PCL with M_n of 10,000 and CALB of 100 mg in toluene. At low substrate concentration, relatively high degradation rate was observed but as PCL concentrations were incrementally increased from 10 to 100 g L^{-1}, initial rates of PCL degradation were decreased. According to Pethrick (1986), a dilute solution is defined as concentration

where the product of the intrinsic viscosity [ŋ] multiplied by the concentration *c*, is less than one. In dilute solution, polymer molecules act primarily as isolated chains, thus increasing the accessibility of the ester bond to CALB attack.

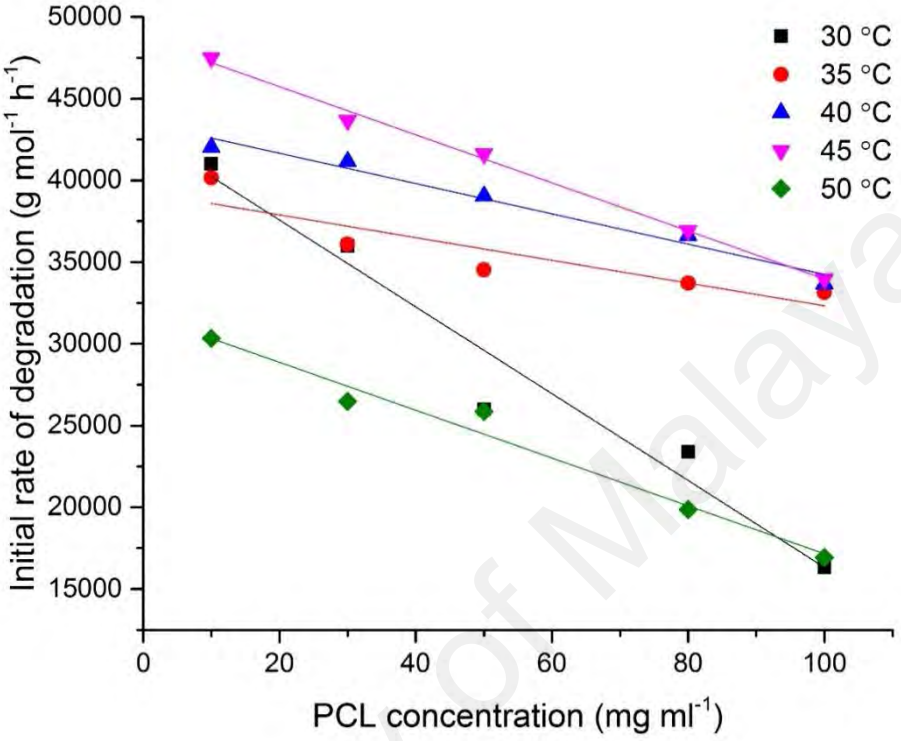

Figure 4.12. Initial rate of hydrolysis as a function of PCL concentration (mg ml^{-1}) and reaction temperature (°C).

From Table 4.5, [ŋ]*c* was proportionately increased when the concentration of PCL increased, and this was hypothesized to result in shrank excluded-volume, giving rise to greater than before inter-molecular interactions between distant part of polymer chains. This restricts access for CALB attacks on the polymer chains. Excluded-volume effect transpired in dilute solution, where polymer chains are well separated, and the segmental interactions are primarily intra-molecular interactions (Pethrick, 1986). As observed in Figure 4.12, despite increasing the reaction temperature, the initial rate of PCL degradation consistently decreased with its increase in concentration.

Table 4.5. Type of PCL solutions at different concentration of solutes.

PCL concentration , c (g L^{-1})	[ŋ] c				Type of solution
	Benzene	Chloroform	Tetrahydrofuran	Average	
10	0.2003	0.2466	0.2411	0.2293	Dilute
30	0.6009	0.7398	0.7233	0.6880	Dilute
50	1.0015	1.2330	1.2055	1.1467	Not dilute
80	1.6024	1.9728	1.9288	1.8347	Not dilute
100	2.0030	2.4660	2.4110	2.2933	Not dilute

[ŋ]: intrinsic viscosity (dL g^{-1}); c : concentration (g L^{-1})

4.5 APPARENT ACTIVATION ENERGY OF PCL HYDROLYSIS BY LIPASE (E_a)

Based on the *k'* values calculated at different temperatures in table SS3, the apparent activation energy for the enzymatic degradation of PCL was estimated using Arrhenius plot. E_a was measured from the slope of the graph *ca.* 45 kJ mol^{-1}, which was consistent with E_a estimated by Dixon and Webb (1979) for enzyme-catalyzed reactions. Using published data of Kumar and Gross (2000), E_a for polymerization of PCL was calculated at 81 kJ mol^{-1}. These results were in agreement with the theory that the formation of ester bond requires higher energy input compared to its breakage. Marten *et al.* (2003) reported that E_a at 200 kJ mol^{-1} was calculated for PCL solid film degradation by lipase from *Pseudomonas* sp., and this was five-folds than its E_a for degradation in toluene (this study). Degradation of solid film is a slow process and involves complex processes starting with water molecules penetrating the amorphous regions within the film, which triggers the enzyme-catalyzed hydrolysis of the ester bond and liberation of products into the media (Wang *et al.*, 2004).

CHAPTER 5

CONCLUSION

The findings from this study detailed salient behavior of lipase-mediated hydrolysis of PCL in toluene. Understanding the fundamental physiognomies of the enzymatic scission of biopolymers such PCL assists in the improvement of platform chemicals production from degradation products. These versatile oligomers can be applied as integral components for processes such as copolymerization or functionalization of valuable compounds such as PCL macromere.

FUTURE RECOMMENDATIONS

The low solubility of PCL in aqueous media is a major drawback in the enzymatic polymer degradation. In this study, toluene was employed both as reaction medium and PCL dissolution for better contact between polymer chain and CALB. Although the behavior of CALB-mediated PCL hydrolysis in toluene has been established in the present study, a number of organic solvents also capable of solubilizing PCL such as dichloromethane, chloroform, tetrahydrofuran, carbon tetrachloride, benzene, cyclohexanone and 2-nitropropane still need to be tested as reaction media. Knowledge on monomer and oligomer release by these solvents are vital to understand the behavior of CALB in organic solvents with different properties. It will lead to improved models for better prediction of polymer degradation behavior. Such models are vital for rational exploration of potential biodegradable polymers.

REFERENCES

Alexander, M. K. (2001). Improving enzymes by using them in organic solvents. *Nature, 409*(6817), 241-246.

Annuar, M. S. M., Tan, I. K. P., Ibrahim, S., & Ramachandran, K. B. (2008). A kinetic model for growth and biosynthesis of medium-chain-length poly-(3-hydroxyalkanoates) in *Pseudomonas putida*. *Brazilian Journal of Chemical Engineering, 25*, 217-228.

Ansari, N., & Amirul, A. A. (2013). Preparation and characterization of polyhydroxyalkanoates macroporous scaffold through enzyme-mediated modifications. *Applied Biochemistry and Biotechnology, 170*(3), 690-709.

Arote, R., Kim, T.-H., Kim, Y.-K., Hwang, S.-K., Jiang, H.-L., Song, H.-H., Nah, J.-W., Cho, M.-H., & Cho, C.-S. (2007). A biodegradable poly(ester amine) based on polycaprolactone and polyethylenimine as a gene carrier. *Biomaterials, 28*(4), 735-744.

Barber, F. A., & Click, J. N. (1992). The effect of inflammatory synovial fluid on the breaking strength of new "long lasting" absorbable sutures. *Arthroscopy: The Journal of Arthroscopic & Related Surgery, 8*(4), 437-441.

Bose, M., Nott, P. R., & Kumaran, V. (2004). Excluded-volume attraction in vibrated granular mixtures. *EPL (Europhysics Letters), 68*(4), 508.

Chen, C. S., Fujimoto, Y., Girdaukas, G., & Sih, C. J. (1982). Quantitative analyses of biochemical kinetic resolutions of enantiomers. *Journal of the American Chemical Society, 104*(25), 7294-7299.

Christopher, X. F. L., Monica, M. S., Swee-Hin, T., & Dietmar, W. H. (2008). Dynamics of in vitro polymer degradation of polycaprolactone-based scaffolds: accelerated versus simulated physiological conditions. *Biomedical Materials, 3*(3), 034108.

Chung, A. S., Hwang, H. S., Das, D., Zuk, P., McAllister, D. R., & Wu, B. M. (2012). Lamellar stack formation and degradative behaviors of hydrolytically degraded poly(ε-caprolactone) and poly(glycolide-ε-caprolactone) blended fibers. *Journal of Biomedical Materials Research Part B: Applied Biomaterials, 100B*(1), 274-284.

Coulembier, O., Degée, P., Hedrick, J. L., & Dubois, P. (2006). From controlled ring-opening polymerization to biodegradable aliphatic polyester: Especially poly(β-malic acid) derivatives. *Progress in Polymer Science, 31*(8), 723-747.

Deniz, K. A., & Chang, L. (2000). Microfabrication technology for polycaprolactone, a biodegradable polymer. *Journal of Micromechanics and Microengineering, 10*(1), 80.

Desai, P. D., Dave, A. M., & Devi, S. (2004). Entrapment of lipase into K-carrageenan beads and its use in hydrolysis of olive oil in biphasic system. *Journal of Molecular Catalysis B : Enzymatic, 31*(4–6), 143-150.

Dixon, M., & Webb, E. C. (1979). *Enzymes* (3rd ed.). New York: Academic Press.

Ebata, H., Toshima, K., & Matsumura, S. (2000). Lipase-catalyzed transformation of poly(ε-caprolactone) into cyclic dicaprolactone. *Biomacromolecules, 1*(4), 511-514.

Elzein, T., Nasser-Eddine, M., Delaite, C., Bistac, S., & Dumas, P. (2004). FTIR study of polycaprolactone chain organization at interfaces. *Journal of Colloid and Interface Science, 273*(2), 381-387.

Engelberg, I., & Kohn, J. (1991). Physico-mechanical properties of degradable polymers used in medical applications: a comparative study. *Biomaterials, 12*(3), 292-304.

Gan, Z., Liang, Q., Zhang, J., & Jing, X. (1997). Enzymatic degradation of poly(ε-caprolactone) film in phosphate buffer solution containing lipases. *Polymer Degradation and Stability, 56*(2), 209-213.

Gan, Z., Yu, D., Zhong, Z., Liang, Q., & Jing, X. (1999). Enzymatic degradation of poly(ε-caprolactone)/poly(dl-lactide) blends in phosphate buffer solution. *Polymer, 40*(10), 2859-2862.

Garcia-Alles, L. F., & Gotor, V. (1998). Lipase-catalyzed transesterification in organic media: solvent effects on equilibrium and individual rate constants. *Biotechnology and Bioengineering, 59*(6), 684-694.

Giri, A., Dhingra, V., Giri, C. C., Singh, A., Ward, O. P., & Narasu, M. L. (2001). Biotransformations using plant cells, organ cultures and enzyme systems: current trends and future prospects. *Biotechnology Advances, 19*(3), 175-199.

Gómez-Bombarelli, R., Calle, E., & Casado, J. (2013a). Mechanisms of lactone hydrolysis in acidic conditions. *The Journal of Organic Chemistry, 78*(14), 6880-6889.

Gómez-Bombarelli, R., Calle, E., & Casado, J. (2013b). Mechanisms of lactone hydrolysis in neutral and alkaline conditions. *The Journal of Organic Chemistry, 78*(14), 6868-6879.

Gopferich, A. (1996). Mechanisms of polymer degradation and erosion. *Biomaterials, 17*(2), 103-114.

Griebenow, K., & Klibanov, A. M. (1996). On protein denaturation in aqueous-organic mixtures but not in pure organic solvents. *Journal of the American Chemical Society, 118*.

Gumel, A. M., Annuar, M. S. M., Chisti, Y., & Heidelberg, T. (2012). Ultrasound assisted lipase catalyzed synthesis of poly-6-hydroxyhexanoate. *Ultrasonics Sonochemistry, 19*(3), 659-667.

Gumel, A. M., Annuar, M. S. M., & Heidelberg, T. (2013). Enzymatic synthesis of 6-O-glucosyl-poly(3-hydroxyalkanoate) in organic solvents and their binary mixture. *International Journal of Biological Macromolecules, 55*(0), 127–136.

Gumel, A. M., Annuar, M. S. M., Heidelberg, T., & Chisti, Y. (2011). Lipase mediated synthesis of sugar fatty acid esters. *Process Biochemistry, 46*(11), 2079-2090.

Gumel, A. M., Aris, M. H., & Annuar, M. S. M. (2015). Modification of polyhydroxyalkanoates (PHAs). In I. Roy & P. M. Visakh (Eds.), *Polyhydroxyalkanoate (PHA) based blends, composites and nanocomposites* (pp. 141-182). Cambridge: The Royal Society of Chemistry.

Gupta, N., Rathi, P., & Gupta, R. (2002). Simplified para-nitrophenyl palmitate assay for lipases and esterases. *Analytical Biochemistry, 311*(1), 98-99.

Halling, P. J. (1984). Effects of water on equilibria catalysed by hydrolytic enzymes in biphasic reaction systems. *Enzyme and Microbial Technology, 6*(11), 513-516.

Halling, P. J. (1994). Thermodynamic predictions for biocatalysis in nonconventional media: Theory, tests, and recommendations for experimental design and analysis. *Enzyme and Microbial Technology, 16*(3), 178-206.

Halling, P. J. (2000). Biocatalysis in low-water media: understanding effects of reaction conditions. *Current Opinion in Chemical Biology, 4*(1), 74-80.

Hoskins, J. N., & Grayson, S. M. (2009). Synthesis and degradation behavior of cyclic poly(ε-caprolactone). *Macromolecules, 42*(17), 6406-6413.

Huang, S. J. (1995). Polymer waste management–biodegradation, incineration, and recycling. *Journal of Macromolecular Science, Part A, 32*(4), 593-597.

Hubackova, J., Dvorackova, M., Svoboda, P., Mokrejs, P., Kupec, J., Pozarova, I., Alexy, P., Bugaj, P., Machovsky, M., & Koutny, M. (2013). Influence of various starch types on PCL/starch blends anaerobic biodegradation. *Polymer Testing, 32*(6), 1011-1019.

Iwata, T., & Doi, Y. (2002). Morphology and enzymatic degradation of poly(ϵ-caprolactone) single crystals: does a polymer single crystal consist of micro-crystals? *Polymer International, 51*(10), 852-858.

Jenkins, M. J., & Harrison, K. L. (2008). The effect of crystalline morphology on the degradation of polycaprolactone in a solution of phosphate buffer and lipase. *Polymers for Advanced Technologies, 19*(12), 1901-1906.

Joshi, P., & Madras, G. (2008). Degradation of polycaprolactone in supercritical fluids. *Polymer Degradation and Stability, 93*(10), 1901-1908.

Kamal, M. Z., Yedavalli, P., Deshmukh, M. V., & Rao, N. M. (2013). Lipase in aqueous-polar organic solvents: Activity, structure, and stability. *Protein Science, 22*(7), 904-915.

Kaufman, M. J. (1990). Rate and equilibrium constants for acid-catalyzed lactone hydrolysis of HMG-CoA reductase inhibitors. *International Journal of Pharmaceutics, 66*(1), 97-106.

Kawata, T., & Ogino, H. (2009). Enhancement of the organic solvent-stability of the LST-03 lipase by directed evolution. *Biotechnology Progress, 25*(6), 1605-1611.

Kobayashi, S. (2010). Lipase-catalyzed polyester synthesis–a green polymer chemistry. *Proceedings of the Japan Academy, Series B, 86*(4), 338-365.

Kobayashi, S., & Makino, A. (2009). Enzymatic polymer synthesis: an opportunity for green polymer chemistry. *Chemical Reviews, 109*(11), 5288-5353.

Kobayashi, S., Uyama, H., & Takamoto, T. (2000). Lipase-catalyzed degradation of polyesters in organic solvents. A new methodology of polymer recycling using enzyme as catalyst. *Biomacromolecules, 1*(1), 3-5.

Kondo, R., Toshima, K., & Matsumura, S. (2002). Lipase-catalyzed selective transformation of polycaprolactone into cyclic dicaprolactone and its repolymerization in supercritical carbon dioxide. *Macromolecular Bioscience, 2*(6), 267-271.

Kula, M.-R. (2008). Introduction. In K. Drauz & H. Waldmann (Eds.), *Enzyme catalysis in organic synthesis* (2nd ed., pp. 1-39). Weinheim, Germany: Wiley-VCH Verlag GmbH.

Kumar, A., & Gross, R. A. (2000). *Candida antartica* lipase B catalyzed polycaprolactone synthesis: effects of organic media and temperature. *Biomacromolecules, 1*(1), 133-138.

Kweon, H. Y., Yoo, M. K., Park, I. K., Kim, T. H., Lee, H. C., Lee, H. S., Oh, J. S., Akaike, T., & Cho, C. S. (2003). A novel degradable polycaprolactone networks for tissue engineering. *Biomaterials, 24*(5), 801-808.

Li, S., Garreau, H., & Vert, M. (1990a). Structure-property relationships in the case of the degradation of massive aliphatic poly-(α-hydroxy acids) in aqueous media. *Journal of Materials Science: Materials in Medicine, 1*(3), 123-130.

Li, S., Garreau, H., & Vert, M. (1990b). Structure-property relationships in the case of the degradation of massive poly(α-hydroxy acids) in aqueous media. *Journal of Materials Science: Materials in Medicine, 1*(4), 198-206.

Li, Y.-F., Rubert, M., Aslan, H., Yu, Y., Howard, K. A., Dong, M., Besenbacher, F., & Chen, M. (2014). Ultraporous interweaving electrospun microfibers from PCL-PEO binary blends and their inflammatory responses. *Nanoscale, 6*(6), 3392-3402.

Lo, H.-Y., Kuo, H.-T., & Huang, Y.-Y. (2010). Application of polycaprolactone as an anti-adhesion biomaterial film. *Artificial Organs, 34*(8), 648-653.

Marten, E., Müller, R.-J., & Deckwer, W.-D. (2003). Studies on the enzymatic hydrolysis of polyesters I. Low molecular mass model esters and aliphatic polyesters. *Polymer Degradation and Stability, 80*(3), 485-501.

Matsumura, S. (2006). Enzymatic synthesis of polyesters via ring-opening polymerization. In S. Kobayashi, H. Ritter & D. Kaplan (Eds.), *Enzyme-catalyzed synthesis of polymers* (Vol. 194, pp. 95-132). Berlin Heidelberg: Springer.

Matsumura, S., Ebata, H., & Toshima, K. (2000). A new strategy for sustainable polymer recycling using an enzyme: poly(ε-caprolactone). *Macromolecular Rapid Communications, 21*(12), 860-863.

Mochizuki, M., Hirano, M., Kanmuri, Y., Kudo, K., & Tokiwa, Y. (1995). Hydrolysis of polycaprolactone fibers by lipase: effects of draw ratio on enzymatic degradation. *Journal of Applied Polymer Science, 55*(2), 289-296.

Mook Choi, W., Wan Kim, T., Ok Park, O., Keun Chang, Y., & Woo Lee, J. (2003). Preparation and characterization of poly(hydroxybutyrate-co-hydroxyvalerate)–organoclay nanocomposites. *Journal of Applied Polymer Science, 90*(2), 525-529.

Paravidino, M., Böhm, P., Gröger, H., & Hanefeld, U. (2012). Hydrolysis and formation of carboxylic acid esters. In K. Drauz, H. Gröger & O. May (Eds.), *Enzyme catalysis in organic synthesis* (Third ed., pp. 249-362). KGaA, Weinheim, Germany: Wiley-VCH Verlag GmbH & Co.

Patrício, T., Domingos, M., Gloria, A., & Bártolo, P. (2013). Characterisation of PCL and PCL/PLA scaffolds for tissue engineering. *Procedia CIRP, 5*, 110-114.

Pethrick, R. A. (1986). Molecular motion in concentrated polymer systems: high-frequency behavior. In W. C. Forsman (Ed.), *Polymers in solution: theoretical considerations and newer methods of characterization* (pp. 239-266). Boston, MA: Springer US.

Pitt, C. G., Andrady, A. L., Bao, Y. T., & Samuel, N. K. P. (1987). Estimation of rates of drug diffusion in polymers. In P. I. Lee & W. R. Good (Eds.), *Controlled-release technology* (Vol. 348, pp. 49-70). Washington, DC: American Chemical Society.

Plackett, D. V., Holm, V. K., Johansen, P., Ndoni, S., Nielsen, P. V., Sipilainen-Malm, T., Sodergard, A., & Verstichel, S. (2006a). Characterization of L-potylactide and L-polylactide-polycaprolactone co-polymer films for use in cheese-packaging applications. *Packaging Technology and Science, 19*(1), 1-24.

Plackett, D. V., Holm, V. K., Johansen, P., Ndoni, S., Nielsen, P. V., Sipilainen-Malm, T., Södergård, A., & Verstichel, S. (2006b). Characterization of l-polylactide and l-polylactide–polycaprolactone co-polymer films for use in cheese-packaging applications. *Packaging Technology and Science, 19*(1), 1-24.

Reed, C. R., Han, L., Andrady, A., Caballero, M., Jack, M. C., Collins, J. B., Saba, S. C., Loboa, E. G., Cairns, B. A., & van Aalst, J. A. (2009). Composite tissue engineering on polycaprolactone nanofiber scaffolds. *Annals of Plastic Surgery, 62*(5), 505-512.

Rentsch, B., Hofmann, A., Breier, A., Rentsch, C., & Scharnweber, D. (2009). Embroidered and surface modified polycaprolactone-co-lactide scaffolds as bone substitute: in vitro characterization. *Annals of Biomedical Engineering, 37*(10), 2118-2128.

Rittié, L., & Perbal, B. (2008). Enzymes used in molecular biology: a useful guide. *Journal of Cell Communication and Signaling, 2*(1-2), 25-45.

Rudd, T., Sterritt, R. M., & Lester, J. N. (1984). Formation and conditional stability constants of complexes formed between heavy metals and bacterial extracellular polymers. *Water Research, 18*(3), 379-384.

Sammon, C., Yarwood, J., & Everall, N. (2000). An FT–IR study of the effect of hydrolytic degradation on the structure of thin PET films. *Polymer Degradation and Stability, 67*(1), 149-158.

Santaniello, E., Ferraboschi, P., & Grisenti, P. (1993). Lipase-catalyzed transesterification in organic solvents: applications to the preparation of enantiomerically pure compounds. *Enzyme and Microbial Technology, 15*(5), 367-382.

Secundo, F., Carrea, G., Soregaroli, C., Varinelli, D., & Morrone, R. (2001). Activity of different *Candida antarctica* lipase B formulations in organic solvents. *Biotechnology and Bioengineering, 73*(2), 157-163.

Segel, I. H. (1976). *Biochemical calculations how to solve mathematical problems in general biochemistry*. New York: Wiley.

Singh, A., Ma, D., & Kaplan, D. L. (2000). Enzyme-mediated free radical polymerization of styrene. *Biomacromolecules, 1*(4), 592-596.

Siracusa, V., Rocculi, P., Romani, S., & Dalla Rosa, M. (2008). Biodegradable polymers for food packaging: a review. *Trends in Food Science & Technology, 19*(12), 634-643.

Stevens, M. P. (2009). *Polymer chemistry: an introduction* (3rd ed.). New York: Oxford University Press.

Sun, H., Mei, L., Song, C., Cui, X., & Wang, P. (2006). The in vivo degradation, absorption and excretion of PCL-based implant. *Biomaterials, 27*(9), 1735-1740.

Tamada, J. A., & Langer, R. (1993). Erosion kinetics of hydrolytically degradable polymers. *Proceedings of the National Academy of Sciences of the United States of America, 90*(2), 552-556.

Uyama, H., & Kobayashi, S. (2006). Enzymatic synthesis of polyesters via polycondensation. In S. Kobayashi, H. Ritter & D. Kaplan (Eds.), *Enzyme-catalyzed synthesis of polymers* (Vol. 194, pp. 133-158). Berlin Heidelberg: Springer

Van Lieshout, M., Peters, G., Rutten, M., & Baaijens, F. (2006). A knitted, fibrin-covered polycaprolactone scaffold for tissue engineering of the aortic valve. *Tissue Engineering, 12*(3), 481-487.

Wang, Q., Yang, Z., Wang, L., Ma, M., & Xu, B. (2007). Molecular hydrogel-immobilized enzymes exhibit superactivity and high stability in organic solvents. *Chemical Communications,* (10), 1032-1034.

Wang, Y.-W., Mo, W., Yao, H., Wu, Q., Chen, J., & Chen, G.-Q. (2004). Biodegradation studies of poly(3-hydroxybutyrate-co-3-hydroxyhexanoate). *Polymer Degradation and Stability, 85*(2), 815-821.

Williamson, M. R., & Coombes, A. G. A. (2004). Gravity spinning of polycaprolactone fibres for applications in tissue engineering. *Biomaterials, 25*(3), 459-465.

Wood, R. D., Raju, P. K., & Reiser, R. (1965). Gas-liquid chromatographic analysis of monoglycerides as their trimethylsilyl ether derivatives. *Journal of the American Oil Chemists' Society, 42*(3), 161-165.

Yadav, G. D., & Devi, K. M. (2004). Immobilized lipase-catalysed esterification and transesterification reactions in non-aqueous media for the synthesis of tetrahydrofurfuryl butyrate: comparison and kinetic modeling. *Chemical Engineering Science, 59*(2), 373-383.

Yang, K. S., Park, S. H., Choi, Y. O., & Cho, C. S. (2002). Fiber formation from semi-interpenetrating polymer networks consisting of polycaprolactone and a poly(ethylene glycol) macromer. *Journal of Applied Polymer Science, 84*(4), 835-841.

Zaks, A., & Klibanov, A. M. (1985). Enzyme-catalyzed processes in organic solvents. *Proceedings of the National Academy of Sciences of the United States of America, 82*(10), 3192-3196.

Zeng, J., Chen, X., Liang, Q., Xu, X., & Jing, X. (2004). Enzymatic degradation of poly(L-lactide) and poly(epsilon-caprolactone) electrospun fibers. *Macromolecular Bioscience, 4*(12), 1118-1125.

PUBLICATIONS AND CONFERENCES

Publications:

1. Gumel, A. M., Aris, M. H., & Annuar, M. S. M. (2015). Modification of polyhydroxyalkanoates (PHAs). In I. Roy & P. M. Visakh (Eds.), *Polyhydroxyalkanoate (PHA) based blends, composites and nanocomposites* (pp. 141-182). Cambridge: The Royal Society of Chemistry.

2. Aris, M. H., Annuar, M. S. M., & Ling, T. C. (2016). Lipase-mediated degradation of poly-ε-caprolactone in toluene: behavior and its action mechanism. *Polymer Degradation and Stability, 133*, 182-191.

Conference(s):

1. International conference ASCENT 2015, FTMS college, Technology Park, Malaysia, Bukit Jalil, Kuala Lumpur

APPENDIX

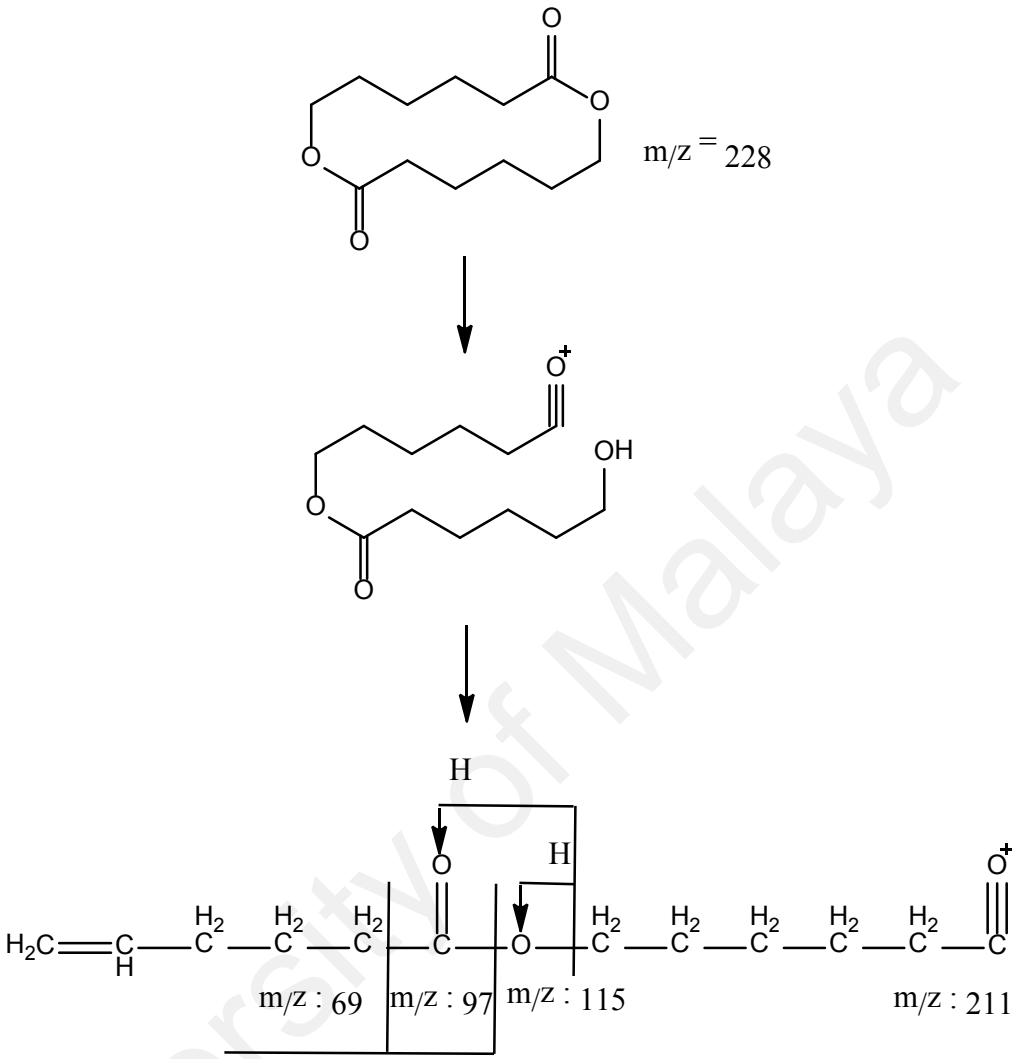

Figure SS1. Chart shows the fragmentation of dicaprolactone by electron impact ionization (EI)

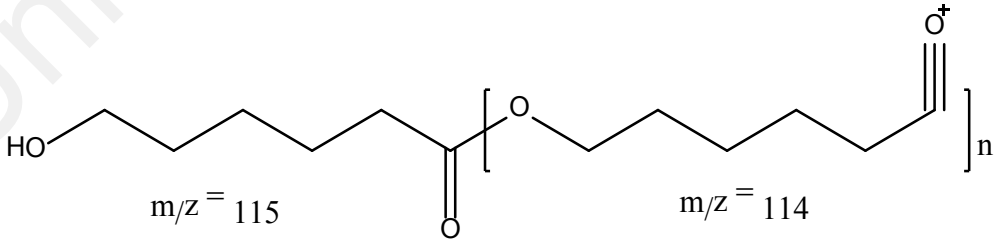

where n = 1, 2, and 3

Figure SS2. Diagram shows the calculation of mass-to-charge ratio for lactone chain

Table SS3 shows the initial rate of degradation at different concentration of PCL

Temperature (K)	Initial rate of degradation (g mol^{-1} h^{-1}) at different concentration of PCL (g mol^{-1})					Rate constant, k' (h^{-1})
	10	30	50	80	100	
303	41009	35994	26009	23392	16330	265.6
308	40150	36092	34535	33719	33139	69.5
313	42042	41164	39054	36639	33656	92.0
318	47503	43660	41623	36912	33972	147.0
323	30333	26479	25864	19868	16921	146.4

Polymer Degradation and Stability 133 (2016) 182–191

Contents lists available at ScienceDirect

Polymer Degradation and Stability

journal homepage: www.elsevier.com/locate/polydegstab

Lipase-mediated degradation of poly-ε-caprolactone in toluene: Behavior and its action mechanism

Muhammad Haziq Aris [a], Mohamad Suffian Mohamad Annuar [a, b, *], Tau Chuan Ling [a]

[a] Institute of Biological Sciences, Faculty of Science, University of Malaya, 50603 Kuala Lumpur, Malaysia
[b] Centre for Research in Biotechnology for Agriculture (CEBAR), University of Malaya, 50603 Kuala Lumpur, Malaysia

ARTICLE INFO

Article history:
Received 11 June 2016
Received in revised form
23 August 2016
Accepted 27 August 2016
Available online 30 August 2016

Keywords:
Poly(ε-caprolactone)
Lipase
Enzymatic degradation
Organic solvent
Cyclic lactones
Scission mechanism

ABSTRACT

Lipase-catalyzed hydrolysis of poly(ε-caprolactone) (PCL) in toulene was investigated. PCL with number-average molecular weight (M_n) 10,000 g mol^{-1} was hydrolyzed using immobilized *Candida antarctica* lipase B (CALB). The increase in PCL concentration led to a decrease in degradation rate. Enhanced rate was observed when reaction temperature was increased from 30 to 50 °C. Enzymatic chain scission of PCL yielded cyclic dicaprolactone, tricaprolactone, tetracaprolactone and oligomers with M_n less than ~1000 g mol^{-1}. Catalytic formation of cyclic lactones *via* back-biting mechanism in low water content environment was attributed to CALB. Its hydrolysis of PCL displayed consecutive random- and chain-end scission with time from detailed thermal, molecular weight and structural analyses. Apparent activation energy, E_a for hydrolysis was 45 kJ mol^{-1} i.e. half of that reverse reaction. Dicaprolactone and oligomers from hydrolysis readily re-polymerized to produce mid-range polymer with M_n 1400 g mol^{-1} after 36 h in the same reaction medium.

1. Introduction

Excellent progress has been made in the application of degradable polymers like poly(ε-caprolactone) (PCL) as tissue-growth scaffolds [1,2], scaffold component for tissue engineering [3–5], anti-adhesion film [6], suture coating [7], drug delivery devices [8] and food packaging [9] because of its biocompatible and non-toxic properties [10] Unlike natural polymer, cells cannot assimilate most synthetic polymers because the degraded products are found to be toxic to them [11,12]. Synthesis of PCL has been performed extensively using various chemical catalysts, while enzymatic synthesis gains extra attention due to its environmental friendly route [4].

It was demonstrated that lipases possess wide substrate specificity with the ability to hydrolyze PCL in aqueous solution [13]. This has been demonstrated in a small scale but has yet to become viable for industrial application because of its low yield, enzyme reusability and cost issues. Furthermore, there is an outstanding issue of the very low solubility of hydrophobic PCL in the aqueous solution [14]. The use of immobilized enzyme for PCL degradation in organic solvent is a promising route in improving reaction kinetic, increasing the yield of degradation products and ease in products separation compared to aqueous mixture [10,15]. More importantly, PCL is more soluble in the organic solvent than aqueous solution.

Single-type, dry organic solvent as reaction medium could be a viable solution to the solubility issue since immobilized enzyme such as CALB still contains about 1 wt % water [14–16] for it to perform degradative catalysis in organic solvent. This nominal amount of water is hypothesized to be sufficient for the enzyme to favor the hydrolysis of PCL as long as aqueous microenvironment on the surface of enzyme is not stripped away by the organic solvent [17]. Trodler and Pleiss [18] reported that non-polar solvent environment resulted in reduced flexibility of CALB in the core and the active site but higher flexibility for residues located on the surface. Proper selection of reaction medium for CALB is very crucial since five surface elements of CALB consisted of a short α-helix (residues 139–150), a long α-helix (residues 266–289) that forms the entrance to the active site, and three surface loops (residues 26–30, 92–97 and 215–222) exhibiting solvent-dependent flexibility change. Non-polar solvents do not alter the backbone and the total surface area of CALB but hydrophilic surface exposure is significantly decreased compared to when CALB is in aqueous environment [18]. The reduction of hydrophilic surface of CALB in

* Corresponding author. Institute of Biological Sciences, Faculty of Science, University of Malaya, 50603 Kuala Lumpur, Malaysia.
E-mail address: suffian_annuar@um.edu.my (M.S.M. Annuar).

http://dx.doi.org/10.1016/j.polymdegradstab.2016.08.015
0141-3910/

CHAPTER 7

Modification of Polyhydroxyalkanoates (PHAs)

A. M. GUMEL, M. H. ARIS AND M. S. M. ANNUAR*

Institute of Biological Sciences, Faculty of Science, University of Malaya, 50603 Kuala Lumpur, Malaysia
*Email: suffian_annuar@um.edu.my

7.1 Introduction

Polyhydroxyalkanoates (PHAs) are biodegradable and biocompatible polyesters with versatile structural compositions. Bacterial PHAs are produced using a combination of renewable feedstock and biological methods mostly *via* a fermentation process. Native and recombinant microorganisms have been generally used to produce different types of PHAs, such as homopolymers[1,2] and copolymers of diverse morphology.[3–5] Alternative production schemes of PHAs *in vitro* based on cell-free enzymatic catalysis are gaining momentum and may become the preferred route to some specialty products.[6,7]

In addition to their biodegradability, compatibility, and compostability, PHAs were reported to possess gas-barrier properties almost similar to those of polyvinyl chloride and polyethylene terephthalate.[8] These combinations of excellent physico–chemical properties coupled with the current concerns over environmental pollution and waste degradation drive their increasing commercial exploitation in different niche applications spanning from biomedical, packaging, automotive, infrastructure, aerospace to military applications.[7,9]

RSC Green Chemistry No. 30
Polyhydroxyalkanoate (PHA) Based Blends, Composites and Nanocomposites
Edited by Ipsita Roy and Visakh P M

Published by the Royal Society of Chemistry, www.rsc.org